

New insights into repolarization analysis

(Ital Heart J 2004; 5 (Suppl 1): 162S-183S)

© 2004 CEPI Srl

RISK STRATIFICATION BY HEART RATE TURBULENCE IN POST-INFARCTION PATIENTS

Petra Barthel, Axel Bauer,
Raphael Schneider, Georg Schmidt

*First Medical Clinic, Klinikum rechts der Isar and
German Heart Center Munich, Munich University
of Technology, Munich Germany*

Heart rate turbulence (HRT) is a measure of the autonomic response to perturbations of arterial blood pressure after single ventricular premature complex (VPC). This response consists of a short initial acceleration followed by a gradual deceleration of the heart rate¹. One of the mechanisms proposed for the genesis of HRT is the alteration in the baroreceptor reflex elicited by the small drop of the arterial pressure due to the VPC. According to this concept, HRT can be non-invasively assessed quasi as “nature’s own autonomic perturbation experiment”².

Quantification of heart rate turbulence

HRT is usually measured from Holter recordings. HRT analysis has also been conducted on event records from implanted cardiac defibrillators. HRT can also be induced by intracardiac pacing in the electrophysiology lab or in patients with implanted cardiac defibrillators. Such HRT has been called “induced HRT”³.

Since the post-extrasystolic fluctuations of RR intervals are in the range of milliseconds and overlaid by heart rate variability of other origin, HRT can only be visualized after averaging of all VPC sequences in a 24-hour Holter ECG. Figure 1A shows such an averaged “local tachogram” of a post-infarction patient who survived the follow-up period of 2 years, figure 1B shows the local tachogram of a patient who suddenly died 3 months after index infarction.

The initial acceleration of heart rate is quantified by the relative change of normal-

to-normal (RR) intervals immediately after and before the VPC and is termed “turbulence onset” (TO). In precise numerical terms the following formula is used: TO is the difference between the mean of the first two sinus RR intervals following the VPC and the last two sinus RR intervals before the VPC divided by the mean of the last two sinus RR intervals before the VPC:

$$TO = \frac{(RR_1 + RR_2) - (RR_{-2} + RR_{-1})}{(RR_{-2} + RR_{-1})} * 100$$

with RR_i being the i -th RR interval following ($i > 0$) the compensatory pause of the VPC or preceding ($i < 0$) the coupling interval of the VPC. These measurements are first performed for each single VPC and subsequently averaged to obtain the value characterizing the patient. $TO > 0\%$ corresponds to sinus rhythm deceleration after a VPC and $TO < 0\%$ to sinus rhythm acceleration after a VPC. The optimal dichotomy for TO is 0% .

The subsequent deceleration of heart rate is quantified by the steepest regression line between the RR interval count and duration. The corresponding parameter is termed “turbulence slope” (TS). In precise numerical terms the following formula is used: TS is the maximum positive slope of a regression line assessed over any sequence of 5 subsequent sinus rhythm RR intervals within the first 15 sinus rhythm RR intervals after a VPC. The value of TS is expressed in milliseconds per RR interval. It was obtained from the tachogram $RR_1, RR_2, RR_3, \dots, RR_{20}$, for each recording, with RR_i being the average of i -th sinus rhythm RR intervals after the compensatory pause of a singular VPC. The optimal dichotomy for TS is 2.5 ms per RR interval.

TO and TS can be used as separate variables or in combination. In the latter case, patients are classified into three HRT categories: category 0, if both TO and TS are normal or if a patient has no VPCs; category 1, if either TO or TS are abnormal; category 2, if both TO and TS are abnormal.

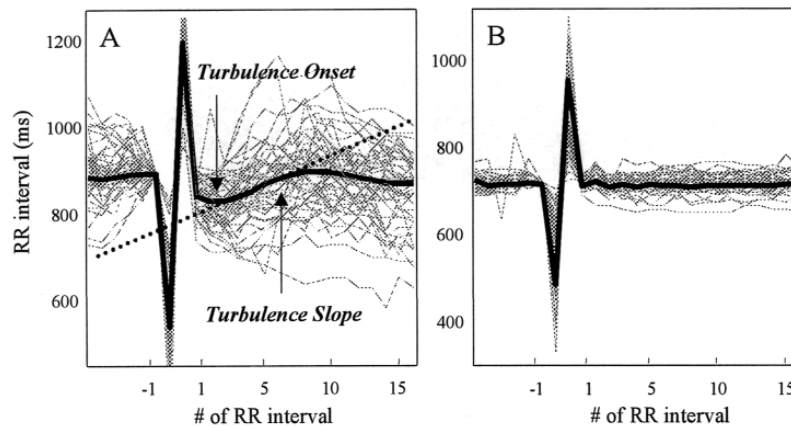


Figure 1. A: signal-averaged tachogram in a post-infarction patient surviving ≥ 2 years. B: signal-averaged tachogram in a post-infarction patient who suddenly died 3 months after the index infarction.

Physiological mechanisms of heart rate turbulence

VPCs are accompanied by both, a lower than normal systolic pulse pressure (due to the reduced stroke volume) and a lower diastolic pressure (due to a longer than normal post-extrasystolic RR interval) (Fig. 2). This perturbation is followed by the HRT pattern of with a latency of < 1 s.

The assumption that a baroreflex mechanism is the driving force of HRT was supported by a series of clinical and experimental studies. Davies et al.⁴ found a strong correlation between HRT and baroreflex sensitivity in a study of 45 patients with chronic heart failure. Later on, this finding was confirmed by Ghuran et al.⁵ who also found a strong correlation between HRT and baroreflex sensitivity in the Autonomic Tone and Reflexes After Myocardial Infarction (ATRAMI) trial cohort. A more theoretical approach was attempted by Mrowka et al.⁶ who

studied HRT in a complex computer model. If the baroreflex was artificially “turned off”, HRT was abolished.

Clinical significance of heart rate turbulence

In the seminal study¹, two major trials in patients with myocardial infarction from the pre-thrombolytic and thrombolytic era were investigated, the Multicentre Postinfarction Program (MPIP) study and the placebo arm of the European Myocardial Infarct Amiodarone Trial (EMIAT). In both MPIP and EMIAT populations, a highly significant association between TO and TS and total mortality during follow-up was found. In EMIAT, TS was the strongest univariate predictor of follow-up mortality while in MPIP, it was the second most powerful univariate predictor of mortality following depressed left ventricular ejection fraction.

The ATRAMI substudy⁵ determined the predictive value of HRT in a low-risk population after acute myocardial infarction. Data were obtained from 1212 survivors with a mean duration of follow-up of 20.3 months. In this study, a composite index of cardiac autonomic function was also assessed by combining HRT (TO and TS), baroreflex sensitivity and the standard deviation of the normal-to-normal RR intervals (SDNN). The study confirmed the independent value of HRT in predicting fatal cardiac arrest and non-fatal cardiac arrest in a low-risk post-acute myocardial infarction population. At the same time, the composite autonomic index (combined TO, TS, baroreflex sensitivity, and SDNN) was the strongest risk predictor.

Barthel et al.⁷ recently published the first prospective study (ISAR-HRT) to validate HRT in a large cohort of the reperfusion era; 1455 survivors of an acute myocardial infarction (age < 76 years) in sinus rhythm were enrolled in this study. HRT was shown to be the strongest ECG-based risk predictor. HRT category 2, i.e.,

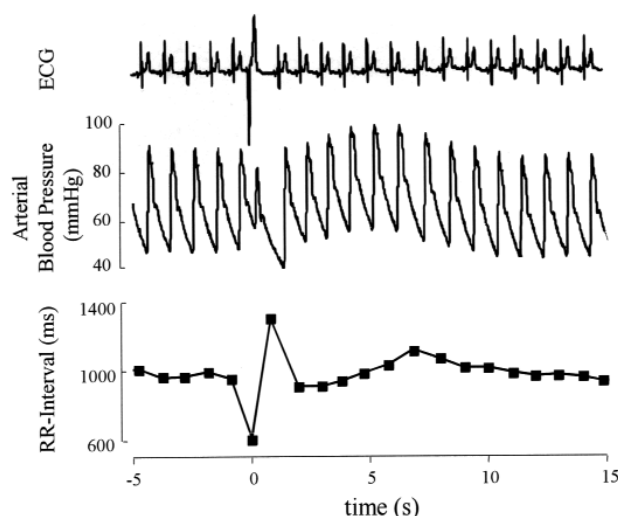


Figure 2. Simultaneous recordings of ECG, arterial blood pressure and RR intervals in a post-infarction patient. Arterial pressure was non-invasively recorded by Finapres®.

the combination of an abnormal TO and an abnormal TS, was as powerful as left ventricular ejection fraction as a risk predictor. HRT category 2 remained highly significant after adjustment for left ventricular ejection fraction and other clinical risk factors. This category indicated a 6-fold risk of death within the first 2 years after myocardial infarction. HRT identified high-risk subgroups in patients with left ventricular ejection fraction ≤ 30 and $> 30\%$. In both subgroups, HRT category 2 was a significant and independent predictor of death.

The clinical characteristics of all major post-infarction studies are summarized in table I, the results of the multivariate analyses are summarized in table II and figure 3.

HRT in patients undergoing direct percutaneous coronary intervention for acute myocardial infarction has also been evaluated prospectively⁸. TO and TS were determined before reperfusion, during the initial 2 hours

after reperfusion, and during hours 6 to 24 after reperfusion. HRT significantly improved after percutaneous coronary intervention in patients with TIMI 3 flow reflecting rapid restoration of baroreceptor response after successful reperfusion. There was persistent impairment of HRT after percutaneous coronary intervention in patients with TIMI 2 flow indicating a sustained blunted baroreflex response and may reflect a more severe microvascular dysfunction.

Conclusions

HRT is a simple and non-invasive method to assess baroreflex function. In post-infarction patients, HRT is a potent risk stratification tool and provides information “on top” of left ventricular function.

Table I. MPIP, EMIAT, ATRAMI and ISAR-HRT: study characteristics, clinical variables and therapy.

	MPIP (n=577)	EMIAT (placebo) (n=614)	ATRAMI (n=981)	ISAR-HRT (n=1455)
Inclusion criteria	Acute MI	Acute MI and LVEF $\pm 40\%$	Acute MI	Acute MI
Primary endpoint	Total mortality 13% (75/577)	Total mortality 14% (87/614)	Cardiac mortality 4.1% (40/981)	Total mortality 4.8% (70/1455)
Follow-up (months)	22	21	20	22
Age (years)	57 \pm 9	61 \pm 9	57 \pm 10*	59 \pm 10
Women (%)	22	15	13*	21
Previous MI (%)	26	26	7*	14
VPC/hour	16 \pm 49	48 \pm 186	14 \pm 61*	15 \pm 71
LVEF (%)	45 \pm 15	30 \pm 9	49 \pm 12*	54 \pm 13
Revascularization (%)	0	60	63*	98
β -blockers	32	44	20*	93

LVEF = left ventricular ejection fraction; MI = myocardial infarction; VPC = ventricular premature complex. * data refer to the 1284 patients of the original ATRAMI population and not to the 981 patients, in which heart rate turbulence was assessable.

Table II. MPIP, EMIAT, ATRAMI and ISAR-HRT: multivariate analyses.

	MPIP (n=577)	EMIAT (placebo) (n=614)	ATRAMI (n=981)	ISAR-HRT (n=1455)
Age ≥ 65 years	–	–	–	2.4 (1.5-3.9)
Diabetes mellitus	Not included	Not included	Not included	2.5 (1.6-4.1)
History of previous MI	–	1.8 (1.2-2.7)	Not included	–
Mean RRI ≤ 800 ms	–	1.8 (1.1-2.9)	–	–
Heart rate variability*	–	–	–	–
Arrhythmia**	–	–	–	–
Baroreflex sensitivity < 3 ms/mmHg	Not available	Not available	–	Not available
LVEF§	2.9 (1.8-4.9)	1.7 (1.1-2.7)	3.5 (1.8-7.1)	4.5 (2.6-7.8)
HRT category 2§§	3.2 (1.7-6.0)	3.2 (1.8-5.6)	4.1 (1.7-9.8)	5.9 (2.9-12.2)

HRT = heart rate turbulence; LVEF = left ventricular ejection fraction; MI = myocardial infarction; RRI = normal-to-normal interval. * heart rate variability index ≤ 20 units (MPIP, EMIAT, ISAR), standard deviation of the normal-to-normal RR intervals < 70 ms (ATRAMI); ** VPC/hour ≥ 10 or non-sustained ventricular tachycardia (MPIP, EMIAT, ISAR), VPC/hour ≤ 10 (ATRAMI); § LVEF $< 30\%$ (MPIP, EMIAT, ISAR), LVEF $< 35\%$ (ATRAMI); §§ abnormal turbulence onset and slope.

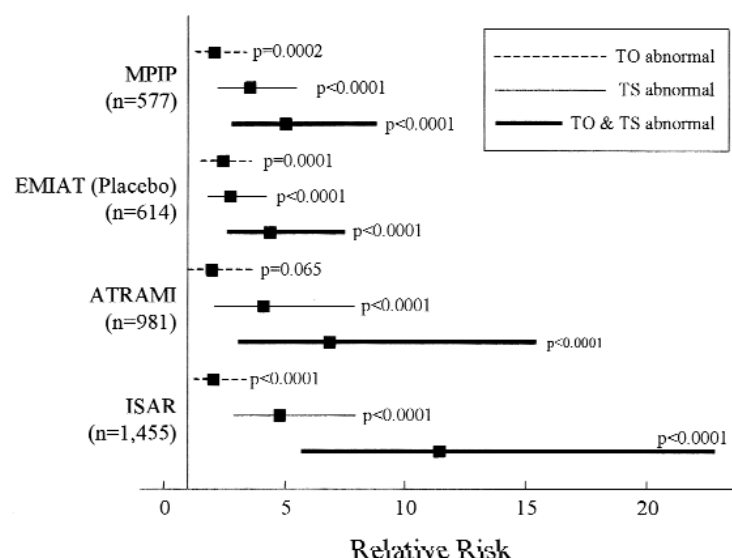


Figure 3. Hazard ratios for total mortality (MPIP, EMIAT and ISAR) and cardiac mortality (ATRAMI) for turbulence onset (TO), turbulence slope (TS) and heart rate turbulence category 2.

References

- Schmidt G, Malik M, Barthel P, et al. Heart-rate turbulence after ventricular premature beats as a predictor of mortality after acute myocardial infarction. *Lancet* 1999; 353: 1390-6.
- Watanabe MA. Heart rate turbulence: a review. *Indian Pacing and Electrophysiology Journal* 2003; 3: 10-22.
- Marine JE, Watanabe MA, Smith TW, Monahan KM. Effect of atropine on heart rate turbulence. *Am J Cardiol* 2002; 89: 767-9.
- Davies LC, Francis DP, Ponikowski P, Piepoli MF, Coats AJ. Relation of heart rate and blood pressure turbulence following premature ventricular complexes to baroreflex sensitivity in chronic congestive heart failure. *Am J Cardiol* 2001; 87: 737-42.
- Ghuran A, Reid F, La Rovere MT, et al. Heart rate turbulence-based predictors of fatal and nonfatal cardiac arrest (The Autonomic Tone and Reflexes After Myocardial Infarction sub-study). *Am J Cardiol* 2002; 89: 184-90.
- Mrowka R, Persson PB, Theres H, Patzak A. Blunted arterial baroreflex causes "pathological" heart rate turbulence. *Am J Physiol Regul Integr Comp Physiol* 2000; 279: R1171-R1175.
- Barthel P, Schneider R, Bauer A, et al. Risk stratification after acute myocardial infarction by heart rate turbulence. *Circulation* 2003; 108: 1221-6.
- Bonnemeier H, Wiegand UK, Friedlbinder J, et al. Reflex cardiac activity in ischemia and reperfusion: heart rate turbulence in patients undergoing direct percutaneous coronary intervention for acute myocardial infarction. *Circulation* 2003; 108: 958-64.

ASSESSMENT OF INDIVIDUAL QT/RR RELATIONSHIP AND HYSTERESIS IN POST-INFARCTION PATIENTS

Esther Pueyo^{*§}, Peter Smetana^{*}, Pablo Laguna[§], Marek Malik^{*}

^{*}Department of Cardiological Sciences, St. George's Hospital Medical School, London, UK, [§]Communications Technology Group, Aragón Institute for Engineering Research (I3A), University of Zaragoza, Spain

In this study the QT interval response to RR interval changes was assessed in 24-hour Holter recordings by considering weighted averages of a history of past RR intervals to characterize the influence of heart rate on each QT measurement. An optimum adaptation profile was individually obtained for each patient, from which several descriptors of the QT/RR hysteresis were derived. Two main results were found in this study: first, the process of QT adaptation to heart rate changes is highly individual and, consequently, any generalized approach may lead to inappropriate conclusions; second, it is important to consider RR interval variations in some previous minutes to completely characterize the QT response.

Introduction

It is known that a time lag exists in the adaptation of the QT interval to RR interval changes. This so-called QT/RR hysteresis is, however, usually ignored in automatic QT analysis of 24-hour Holter recordings. Only simple approaches have been implemented in some Holter systems but always assuming that the duration of the QT/RR hysteresis lag is constant in all patients. In addition, not only the duration but also the way in which QT adapts may substantially differ between subjects. Among others, the omission of the individual adaptation characteristics might result in significant errors in the estimation of heart rate corrected QT interval (QTc).

In this study we investigated the QT/RR hysteresis by analyzing the dynamic dependence of the QT interval behind heart rate changes. In order to relate each QT not only to the immediately preceding RR interval but to a history of previous RR intervals, we considered RR averaging windows preceding each QT measurement. A searching was performed for the window that led to the optimum [QT_i, RR_i] fit, where RR_i is the weighted

average of preceding RR measurements. From the individually derived QT/RR adaptation pattern, the hysteresis lag was numerically quantified and a characterization of the time course of the QT response to heart rate changes was obtained in terms of velocity and profile of the adaptation process.

Methods

Study population. The study investigated a population of 866 patients taken from the EMIAT trial database¹. All subjects were survivors of acute myocardial infarction, aged ≤ 75 years, with left ventricular ejection fraction $\leq 40\%$. Recordings available for the study were 24-hour 3-lead Holter ECGs obtained 1 month after treatment randomization; 462 were obtained on amiodarone and 404 on placebo.

Data analysis. RR and QT intervals were automatically measured on a beat-to-beat basis using a commercial Holter system (Pathfinder, Reynolds Medical Inc.). In each lead, only beats with accepted QT and RR intervals were considered and, in each recording, the lead with more accepted measurements was selected. Detection of incidences in the RR signal (false positives, false negatives and ectopic beats) was carried out according to the methodology described by Mateo and Laguna². Beats for which a preceding 300 s window included no valid measurements were rejected.

QT adaptation pattern. QT interval dependence on preceding RR intervals was characterized by an RR interval averaging window that was optimized to lead to the lowest regression residual of the [QT, RR] data, where \overline{RR} is the corresponding weighted average of RR interval measurements in the window. In order to determine such an optimum weight distribution individually, a global optimization algorithm based on the direct method^{3,4} was implemented, in which the objective function to be minimized was defined at each weight vector $w = (w_1, \dots, w_n)$ as the global residual from fitting any of 10 *a priori* selected regression models⁵ to the [QT_i, RR_i] data, with RR_i computed for each *i*th beat as

$$\overline{RR}_i = \sum_{j=i-N+1}^i w_{j-i+N} RR_j$$

where *N* is the number of beats contained in preceding 300 s window within the 24-hour recording, and $w = (w_1, \dots, w_n)$ are all positive and normalized such that

$$w_1 + \dots + w_n = 1.$$

As a result, 10 different combinations of weights w_i and regression parameters were determined for each recording, each combination characterizing the optimum RR influence associated with one regression

model. A unique pattern of averaging window was identified by selecting the model leading to the minimum residual when the RR intervals were computed from the original RR interval measurements with the regression model-specific optimum weights.

QT/RR descriptors. The assessment of QT adaptation to RR changes described in the previous paragraph provided an individual profile of the QT/RR hysteresis, from which two parameters characterizing the adaptation process were calculated:

- lag, describing the effective length of RR influence. It was computed from the optimum weight distribution w_j by considering a cumulative sum

$$H(j) = \sum_{k=1}^j w_k, j = 1, \dots, N$$

reaching a threshold $\eta = 0.1$ defined to cover 90% of the adaptation (Fig. 1). The number of beats required to achieve the limit imposed by η were counted and lag was defined as the corresponding time in seconds, using the mean RR for conversion from beats to seconds;

- λ , inverse beat-velocity of the QT adaptation. It was determined from fitting the cumulative sum of weights $H(j)$ with an exponential model: $H(j) = e^{Aj+B}$ (Fig. 2). Correlation values > 0.91 confirmed the suitability of the fit. The λ parameter was defined as the time constant of the model: $l = 1/A$.

Heart rate correction. Each of the 10 regression models was converted into a heart rate correction formula by projecting the QT interval onto a standard level of $\overline{RR} = 1$ s. For each patient, the individualized QT correction formula was selected corresponding to the optimally determined regression model. Such a formula was optimized according to the criterion of null Pearson correlation coefficient between QTc and \overline{RR} .

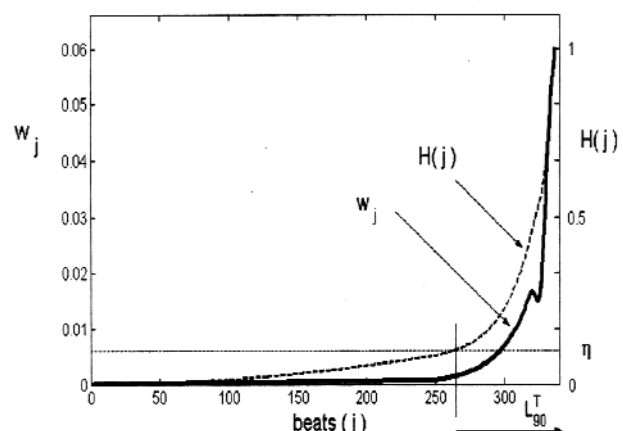


Figure 1. Determination of the effective window length for RR averaging, considering a threshold η covering 90% of the sum of weights. The weight distribution w_j is plotted as a solid line and its cumulative sum $H(j)$ as a dashed line.

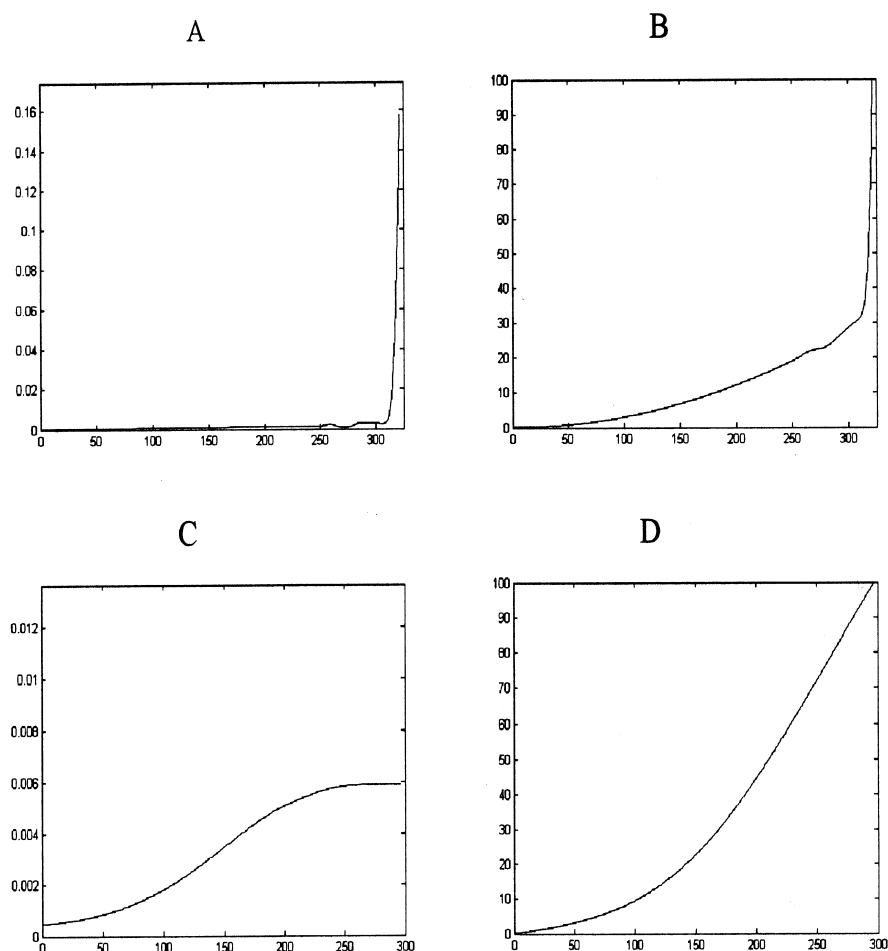


Figure 1. In A and C, two different examples of optimum weight distributions corresponding to 2 patients in the study are represented. Their respective cumulative sums of weights are plotted in B and D, which were fitted with exponential models in order to extract values of the adaptation rate ($\lambda = 46.52$ and $\lambda = 54.67$ beats, respectively).

Results

Quantification of the QT hysteresis lag revealed that, on average, 140 s of the preceding RR intervals have influence on the QT interval duration. Nevertheless, observation of weight distributions characterizing the adaptation profiles showed that the influence of the most distant RR intervals is small compared to the most recent ones. This proportion was differently expressed in different patients.

Examining the individual values of the parameter lag, we observed high intersubject variability, as confirmed by the high standard deviation of the variable, which was around 35 s. In fact, the lag values ranged from 3 to > 215 s.

High intersubject variability was observed not only in the delays of the heart rate adaptation of ventricular repolarization but also in the characteristic adaptation profiles, that is the way in which QT reacts to RR changes. Mean value of λ was 47.6 ± 8.1 beats. Figure 2 shows in panels A and C two examples representative of very different adaptation profiles, with $\lambda = 46.52$ beats characterizing a fast adaptation, and $\lambda = 54.67$ beats

characterizing much slower adaptation, as it can be corroborated by observation of their respective cumulative sums of weights shown in panels B and D.

Results obtained from the present study demonstrate the necessity of considering the individual QT/RR hysteresis patterns and the use of an individualized correction formula to correct the QT interval for the effects of heart rate.

Discussion and conclusions

The evaluation of the QT/RR hysteresis lag developed in this work showed that, despite the strong dependence of QT on the preceding cardiac cycle, an individually variable history of heart rate also contributes to QT variations.

The mode in which previous RR intervals influence each QT measurement and the time interval necessary to describe the complete adaptation process varies significantly among patients. This fact enhances the importance of having obtained individual adaptation profiles representative of optimum weights assigned to past RR

measurements, which should be taken into account within Holter systems. The results of this study clearly disagree with the assumption of the lag in the QT adaptation being constant for all subjects.

References

1. Julian DG, Camm AJ, Frangin G, et al. Randomised trial of effect of amiodarone on mortality in patients with left-ventricular dysfunction after recent myocardial infarction. EMIAT. *Lancet* 1997; 349: 667-73.
2. Mateo J, Laguna P. Analysis of heart rate variability in the presence of ectopic beats using the heart timing signal. *IEEE Trans Biomed Eng* 2003; 50: 334-43.
3. Jones DR, Perttunen CD, Stuckman BE. Lipschitzian optimization without the Lipschitz constant. *Journal of Optimization Theory and Applications* 1993; 79: 157-81.
4. Lewis RM, Torczon V, Trosset MW. Direct search methods: then and now. *Journal of Computational and Applied Mathematics* 2000; 124: 191-207.
5. Pueyo E, Smetana P, Hnatkova K, Laguna P, Malik M. Time for QT adaptation to RR changes and relation to arrhythmic mortality reduction in amiodarone-treated patients. In: Murray A, Arzbaeher R, eds. *Computers in cardiology*. Memphis, TN: IEEE Computer Society Press, 2002: 565-8.

INDIVIDUALIZED CORRECTION OF QT/RR INTERVAL FOR HEART RATE

Velislav Batchvarov, Katerina Hnatkova, Marek Malik

Department of Cardiological Sciences, St. George's Hospital Medical School, London, UK

While in clinical practice, the standard imprecision of heart rate correction of the QT interval (QTc) by Bazett formula seems to be acceptable, investigations that require accurate assessment of QTc values are frequently substantially affected by this imprecision. In particular, studies of drug-induced QT interval prolongation may lead to completely erroneous conclusions if utilizing imprecise *ad hoc* selected heart rate corrections of QT interval. For this reason, the so-called individual heart rate correction approaches have been developed and shown to be superior to the application of any of the previously published correction formulae.

The article reviews the background of the problem and discusses the scientific evidence that was used as the background of the development of individualized heart rate corrections. Clinical utilities of the technology are discussed.

Introduction

Prolongation of the heart rate-corrected QT interval (QTc) is an established risk factor for cardiac and arrhythmic death in the general population and various patient groups¹⁻⁵. In recent years, the interest in the QTc interval has been additionally fueled by the

increased awareness that many cardiac as well as non-cardiac drugs have the potential to affect ventricular repolarization and induce a potentially lethal torsades de pointes (TdP) ventricular arrhythmia⁶. With most drugs administered at standard clinical doses, TdP is rather rare and occurs exclusively in the presence of predisposing conditions, such as heart failure, bradycardia or electrolyte disbalance and/or in susceptible individuals (i.e. asymptomatic carriers of "silent" mutations of long QT syndrome genes^{7,8}). Therefore the absence of cases of TdP in clinical program of drug development is not reassuring. The initial post-marketing surveillance of some drugs that were later withdrawn from the market because of clear proarrhythmic toxicity, was both substantial and signal-free⁹. Therefore the assessment of drug-induced changes of cardiac repolarization needs to be based on surrogate markers of which the most important is the prolongation of the QTc interval. If in addition to the QT interval the investigated drug changes also heart rate, either directly or indirectly through therapeutic actions, the appropriate QT heart rate correction becomes very important.

The precision requirements of the QTc interval measurement are different in clinical practice and in risk stratification and/or drug studies. In clinical practice, an imprecision of 10 to 20 ms, or perhaps even more is less likely to lead to incorrect management decisions since all borderline findings are always interpreted within the context of other clinical findings. On the contrary, errors of 10 ms or even lower may be misleading in drug studies and risk stratification trials (e.g. when selecting patients for a prospective intervention), especially when introduced in a biased way due to systematic differences in heart rate.

The fact that the relative duration of cardiac systole changes with heart rate has been recognized even before the invention of electrocardiography¹⁰. For example, Thurston¹¹ used sphygmographical tracings of the radial pulse to measure the length of the cardiac systole at different heart rates. He confirmed that "the length of the systole of the heart, as indicated in the radial artery, is constant for any given pulse rate, and varies as the cube root of the rapidity". Earlier, Garrod¹² analyzed sphygmographic recordings of the apex beat in healthy subjects and came to the conclusion that "in health, the length of the first part of the heart beat varies ... inversely as the square root of the rapidity". In other publications the same author observed that "the length of the interval between the commencement of the primary and diastolic rises (of the sphygmogram) is constant for any given pulse rate, and varies as the cube root of the pulse rate ..."¹³.

Following the discovery of electrocardiography, the relationship between mechanical systole and the QT interval was studied extensively and the relationship between the QT and RR intervals has been researched ever since.

Unfortunately, despite all the research work spanning over more than one century, the problem of the appropriate heart rate correction of the QT interval has not been

solved. Tens of heart rate correction formulae have been proposed¹⁴ – already in 1949 about 30 such formulae have been described¹⁵, but none of these has been found universally applicable¹⁵⁻²⁰.

It has been repeatedly pointed out that the validity of any formula expressing the QT interval as a function of the simultaneously measured RR interval is limited by physiologic factors, such as the extra-heart rate influences on the QT interval duration²¹⁻²³ (Fig. 1) and the “lag hysteresis” of the QT interval^{24,25} (Fig. 2). Significantly less attention has been paid to the variations of the QT/RR relationship between different individuals as a potential source of error.

Interindividual variations in the QT/RR relationship

While studying different groups of cardiac patient and/or healthy subjects, different authors often reported substantially variable results even when using the same



Figure 1. Direct effect of the autonomic nervous system on the QT interval duration. Each panel shows QT intervals recorded at during the night (thin lines, above) and during the day (thick lines, below) at identical heart rates of 61 b/min (top panel), 65 b/min (middle panel) and 70 b/min (bottom panel). QT intervals recorded during the night are clearly longer than those recorded during the day despite identical heart rates.

form of generic formula to describe the QT/RR relationship. For instance, with the most popular parabolic formula $QT_c = QT/RR^\alpha$ (RR interval expressed in seconds), the reported values of optimum parameter α ranged from 0.25²⁶ to 0.6²⁷ and included the formulae of Bazett ($\alpha = 0.5$)²⁸ and Fridericia ($\alpha = 0.333$)²⁹. Similar disagreement exists between the results of studies using the linear formula $QT_c = QT + \alpha \times (1-RR)$ ^{15,30-32} as well as other types of generic heart rate correction formulae³³⁻³⁵. These discrepancies have been mainly attributed to different types of databases (pooled data of different subjects, multiple recordings in each subject, or mixture of both, as in the original study of Bazett), different physiological conditions (rest, exercise ECGs, various autonomic maneuvers, continuous ambulatory recordings), various heart rates, and different number of ECG samples in the different studies.

Surprisingly little attention has been paid to the possibility that there might be no universal, applicable to all subjects “physiological” QT/RR relationship and that even under identical or comparable conditions different individuals might follow different pattern of adaptation of the QT interval to changes in heart rate.

At the same time, substantial variability in QT/RR relationship has been repeatedly observed in different studies that have collected sufficient data to characterize individual QT/RR patterns. To reliably investigate the individual QT/RR relationship, multiple serial ECGs recorded in the same subject over a wide range of heart rate are needed, either in the form of frequently repeated recordings or in the form of continuous ambulatory

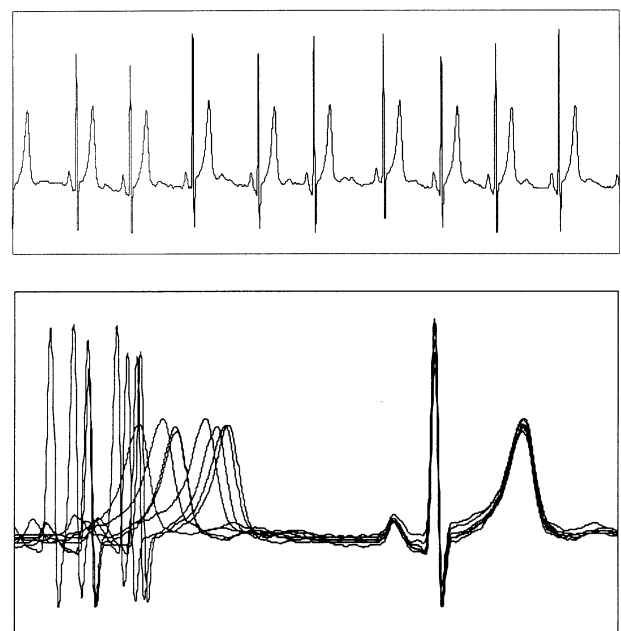


Figure 2. An example of hysteresis of the QT interval. Top panel: 10 s ECG recording during which 8 RR intervals are visibly variable. Bottom panel: all 8 RR intervals have been overlapped and aligned by the R-peak of the second QRS complex. It can be seen that QT intervals preceded by very different RR intervals are almost identical, i.e. they have not yet adapted to the changes in the RR interval.

ECG recordings. In both cases, accurate QT interval measurement in multiple cardiac cycles is also needed.

Several studies demonstrated the advantages of an "individualized" approach to the heart rate correction of the QT interval. Davey³⁶ estimated the slope of the individual QT/heart rate linear regression from multiple QT/RR data points during exercise stress test in healthy subjects and patients with hypertrophic cardiomyopathy and heart failure. In each participant, he also obtained corrected QT intervals by extrapolating the QT/heart rate regression to the heart rate of 60 b/min. These "individual" QTc values separated the three study groups better than the Bazett corrected QTc interval and, unlike the latter, were not correlated with heart rate.

Using multiple QT/RR data from standard Holter recordings in 21 healthy subjects, Molnar et al.³⁷ compared 5 correction formulae with individually optimized formulae derived from the data of each patient. The authors reported that the individual optimizations were superior to conventional heart rate corrections.

A systematic analysis of the interindividual variations of the QT/RR relationship was reported by Malik et al.³⁸ in 2002. The authors investigated ECG data of 25 healthy women (age 31.1 ± 9.9 years) and 25 men (age 36.0 ± 8.6 years). In each subject, one 10 s 12-lead ECG was obtained every 2 min over 24 hours (671 ± 58 recordings per subject) using 12-lead ambulatory digital ECG recorder (SEER MC, GE Medical Systems, Milwaukee, WI, USA). In each individual, the 24-hour sequence of QT/RR data points was fitted with six different two-parameter regression models included the linear ($QT = \beta + \alpha \times RR$), hyperbolic ($QT = \beta + \alpha/RR$) and parabolic ($QT = \beta \times RR^\alpha$) model. The individually optimized values of the α coefficient of each regression model were used to derive individually optimized formulae for heart rate correction of the QT interval.

The pattern of QT/RR scatterplots differed substantially between different subjects (Fig. 3)³⁸. With all models, both coefficients α and β varied substantially between the participants. With the parabolic model, for

example, the coefficient α varied between 0.23 and 0.49, i.e. some subjects followed the prediction of the Kawataki formula ($\alpha = 0.25$), some subjects the prediction of the Fridericia formula ($\alpha = 0.33$), and one extreme subject was near to the prediction of the Bazett formula ($\alpha = 0.5$). The study clearly showed that no "physiological" QT/RR relationship exists that is common to all subjects. Consequently, no "optimum" heart rate correction can be derived that would permit accurate comparisons of QT intervals recorded in different individuals over a wide range of heart rates. For example, correcting a QT interval of 360 ms recorded at 75 b/min with a parabolic formula $QTc = QT/RR^\alpha$, the range of exponent α of 0.23-0.49 represents a range of QTc interval values of 379-401 ms, i.e. differences of up to 22 ms. At 85 and 95 b/min, these QTc differences increase to 36 and 49 ms, respectively (Fig. 4)³⁸.

Stability of the individual QT/RR relationship

In order to use individually optimized heart rate correction formula derived separately in each subject from their QT/RR relationship, the individual pattern of this relationship must be stable over time, i.e. it must vary significantly less within each individual than between different individuals. While methods for individual correction of the QT interval previously have been proposed, as already mentioned³⁷, the concept of the stability of the individual QT/RR pattern has not been investigated or even formulated until very recently.

Lecocq et al.³⁹ studied the QT/RR relationship of 11 subjects at rest, during exercise and after intravenous isoproterenol, and in 12 subjects at rest and after oral propranolol. An exponential model $QT = A - B \times e^{-k \times RR}$ was fitted to the individual QT/RR data. Four of the subjects participated in different parts of the study (10 months apart). When comparing the individual equations from both parts of the study, the authors briefly mentioned that they "... could not find any significant change between the two periods".

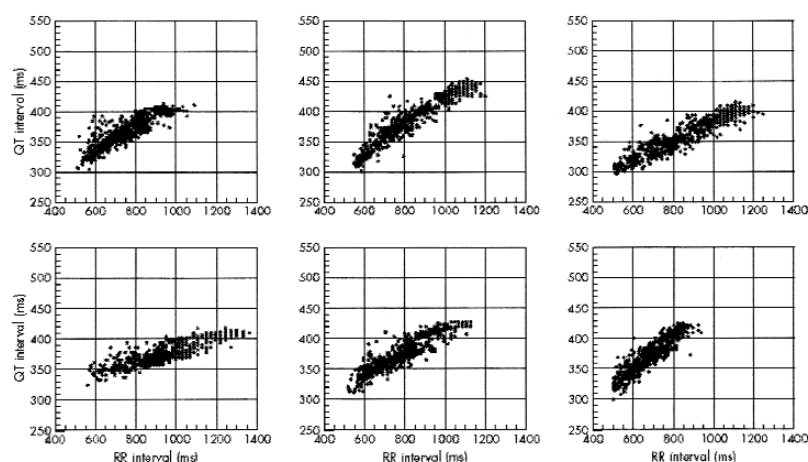


Figure 3. Examples of 24-hour QT/RR relationship patterns in 6 healthy subjects. Note the individual differences. See the text for details. From Malik et al.³⁸, with permission.

Recently, Batchvarov et al.⁴⁰ investigated the individual QT/RR relationship in healthy volunteers. Twenty-four-hour 12-lead digital ECG recordings were obtained at baseline, after 24 ± 0 hours, 7.7 ± 2.0 days, and 31.2 ± 3.9 days in 46 healthy subjects (22 men, 24 women, aged 26.8 ± 7.3 years and 27.3 ± 8.1 years, respectively, $p = \text{NS}$). In each 24-hour recording, one 10 s ECG was obtained every 30 s (1504 ± 283 ECGs per recording). To improve the accuracy of automatic QT measurement, each QT interval was measured using six different algorithms. The QT measurement was accepted if the results with the six algorithms differed by ≤ 40 ms. The mean of the six measurements was taken as the true value of the QT interval (visual control and/or manual editing was impossible since the study involved $> 750\,000$ ECGs). In each recording of each individual, the QT/RR relationship was investigated using 10 different two-parameter regression models, including the linear ($QT = \beta + \alpha \times RR$), hyperbolic ($QT = \beta + \alpha/RR$), parabolic log/log ($QT = \beta \times RR^\alpha$), logarithmic ($QT = \beta + \alpha \times \ln(RR)$) and exponential ($QT = \beta + \alpha \times e^{-RR}$) models.

To compare the intra- and intersubject variability of the regression parameters, the standard deviations of curvature-describing parameter α and the slope-describing parameter β of the 4 consecutive recordings in each participant were compared with the standard deviation of the subject-specific mean values of α and β with a non-parametric one-sample Wilcoxon test.

The shape of the 24-hour QT/RR scatter plots clearly suggested that the QT/RR relationship exhibit substantial intrasubject stability and intersubject variability both in women as well as in men (Fig. 5)⁴⁰.

With all QT/RR regression models, the individual standard deviations of both regression parameters were

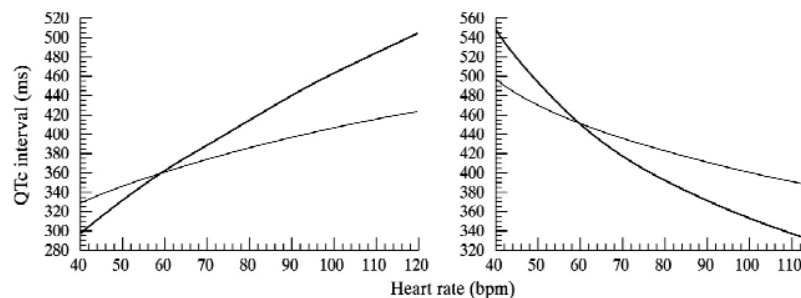


Figure 4. Effect of different values of the curvature coefficient α of the generic correction formula $QTc = QT/RR^\alpha$ on the heart rate-corrected QT interval. This study found coefficient α in a group of healthy subjects ranging from 0.233 to 0.485. The figure shows the differences between the correction formulae $QTc = QT/RR^{0.233}$ (grey lines) and $QTc = QT/RR^{0.485}$ (black lines). For both formulas, the left panel shows the QTc values corresponding to a QT interval of 360 ms measured at different heart rates. The right panel shows “normality limits” – that is, QT interval durations that, when measured at different heart rates, correspond to QTc 450 ms. See the text for details. From Malik et al.³⁸, with permission.

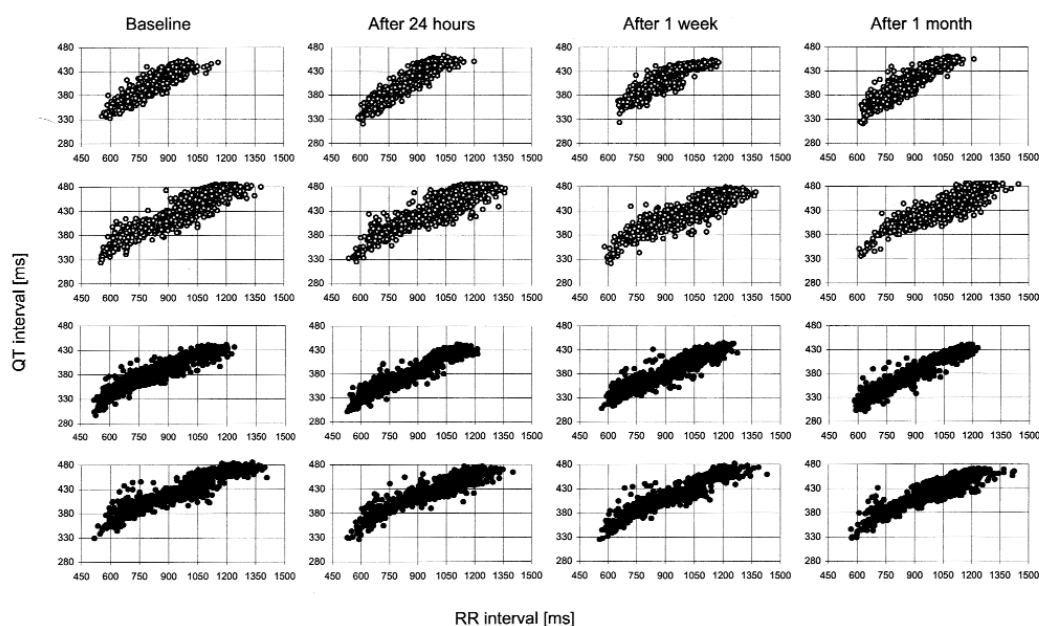


Figure 5. Examples of QT/RR patterns of the four recordings in 2 female (top two rows: open circles) and 2 male subjects (bottom two rows: closed circles). Each row presents the four recordings of one subject, while the four columns present the first and the subsequent recordings of all subjects, respectively. Note the stability of the QT/RR pattern in each subject and the variability of the patterns in different subjects. From Batchvarov et al.⁴⁰, with permission.

highly significantly smaller than the standard deviations of the means of the individual subjects ($p = 10^{-5} - 10^{-9}$; Fig. 6)⁴⁰.

In order to assess the long-term stability of the individual QT/RR relationship, an additional (5th) 24-hour ECG recording was acquired in 16 of the participants in the original study (8 men, age 26.1 ± 7.4 years) after 21.5 ± 5.6 months using the same recording technique⁴¹. Automatic QT measurement and analysis of the QT/RR relationship was performed using the same methods as in the original study. Figure 7 shows examples of QT/RR relationship patterns from recordings taken at baseline, after 1 month and after approximately 2 years in 2 women and 2 men. The long-term stability of the individual QT/RR relationship pattern is clearly visible. The individual standard deviations (from 5 consecutive recordings) of the regression parameters again were significantly smaller ($p < 0.01$) than the standard deviations of the means of the individual subjects. Figure 8 shows comparison of the inter- and intrasubject variability of the regression parameters with the linear (left column) and parabolic (right column) models. The upper panels present the mean \pm SD of the first 4 (open circles) and the fifth recording (closed circles). The bottom panels present mean \pm SD of the regression parameters of the 5 recordings in each subject. It is visible that although the parameters of the fifth recording are different from the first 4, the intersubject variability (lower panels) is substantially higher than the intra-subject variability (top panels).

Individualized heart rate correction

The goal of the application of any heart rate correction formula is to provide QTc interval values that are independent of heart rate.

It is widely assumed that when analyzing a standard clinical ECG with only few ECG complexes recorded at physiological heart rates (e.g. 50-70 b/min), most published heart rate correction formulae provide clinically satisfactory results¹⁶. Our data suggest that in such a scenario Fridericia formula is superior to Bazett formula, since in most healthy subjects the optimum curvature coefficient (parameter α) with the parabolic QT/RR model ($QT = \beta \times RR^\alpha$) is close to 0.33 (Fig. 6)^{38,40}.

However, when more precise estimation of QTc interval is required, such as in drug trials or risk stratification studies, an arbitrarily chosen heart rate correction formula most probably will not respect the individual QT/RR pattern of the majority or of substantial proportion of all patients or healthy subjects. In such cases, Bazett or even Fridericia formulae may provide misleading results even at physiological resting heart rates (e.g. 60-90 b/min)⁴¹ (Fig. 9).

The resulting under- or overcorrection of the QT intervals may lead to substantially misleading results. In

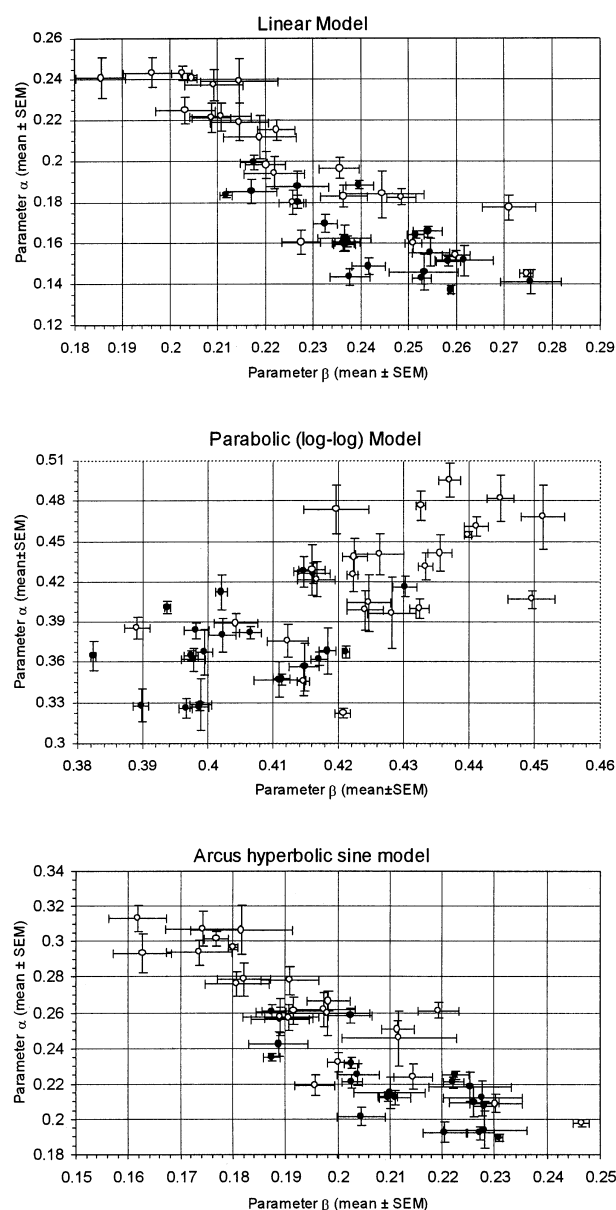


Figure 6. Mean \pm SEM from the four recordings of the α and β parameters of each male (closed circles) and female (open circles) subject with the linear (top panel), parabolic (middle panel) and arcus hyperbolic sine (bottom panel) QT/RR regression model. Note that the standard errors of the individual means are substantially smaller than the range of the individual means. See the text for details. From Batchvarov et al.⁴⁰, with permission.

such studies, an individually optimized heart rate correction formula should be derived in each subject from multiple ECG recordings taken in baseline state. Moreover, in drug studies, the individual baseline and/or placebo QT/RR pattern may be compared with the on-treatment pattern in the same subject.

This concept was applied in a recent study by Malik¹⁴ who investigated data from a phase I study of non-sedating antihistamines ebastine and terfenadine in healthy volunteers. The effectiveness of three different heart rate correction methods to detect drug-induced QT interval prolongation was compared. Firstly, the QT intervals were corrected using 20 previously published heart rate cor-

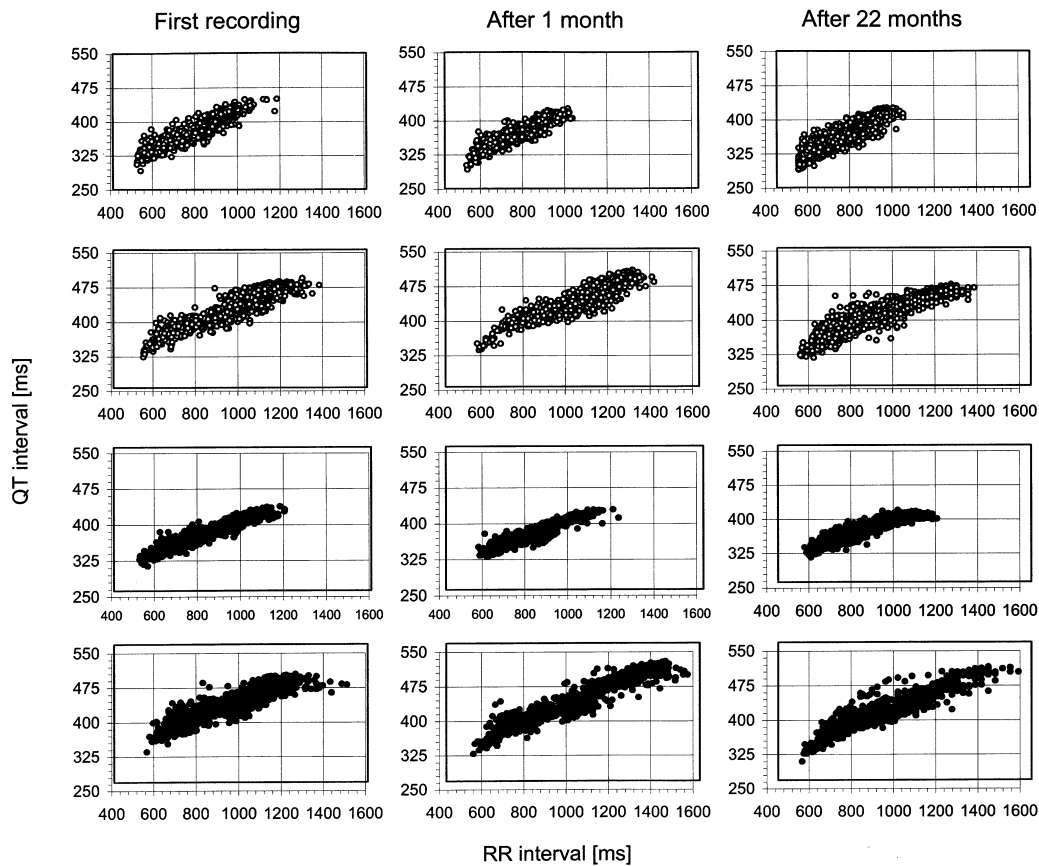


Figure 7. Examples of QT/RR patterns of recordings acquired at baseline (left column), after 1 month (middle column) and after approximately 22 months (right column) in 2 women (top 2 rows, open circles) and 2 men (bottom 2 rows, closed circles). The intersubject variability and the intrasubject stability of the QT/RR relationship are clearly visible.

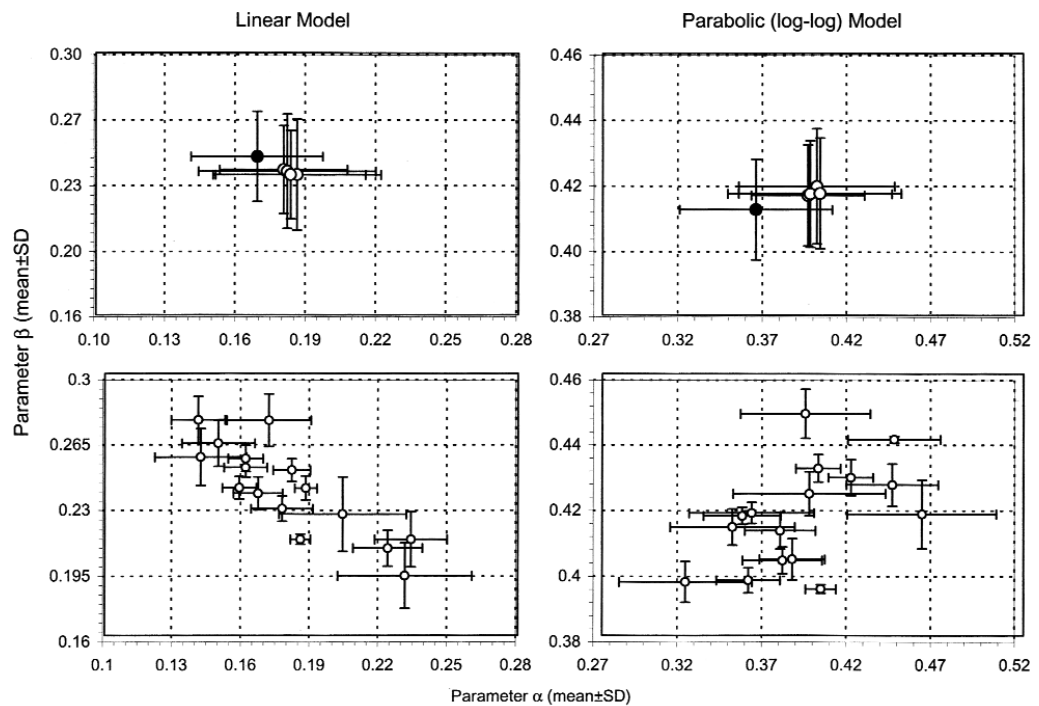


Figure 8. Comparison of the inter- and intrasubject variability of the regression parameters α and β with the linear (left column) and logarithmic (right column) models. The upper panels present the mean \pm SD of α and β of all subjects of the first four (open circles) and of the fifth recording (closed circle). The bottom panels present mean \pm SD of α and β of the five recordings in each subject. It is visible that while the parameters of the fifth recording are different from the first four, the intersubject variability (lower panels) is substantially higher than the intrasubject variability (top panel). Note that unlike figure 6, data in this figure are presented as mean \pm SD.

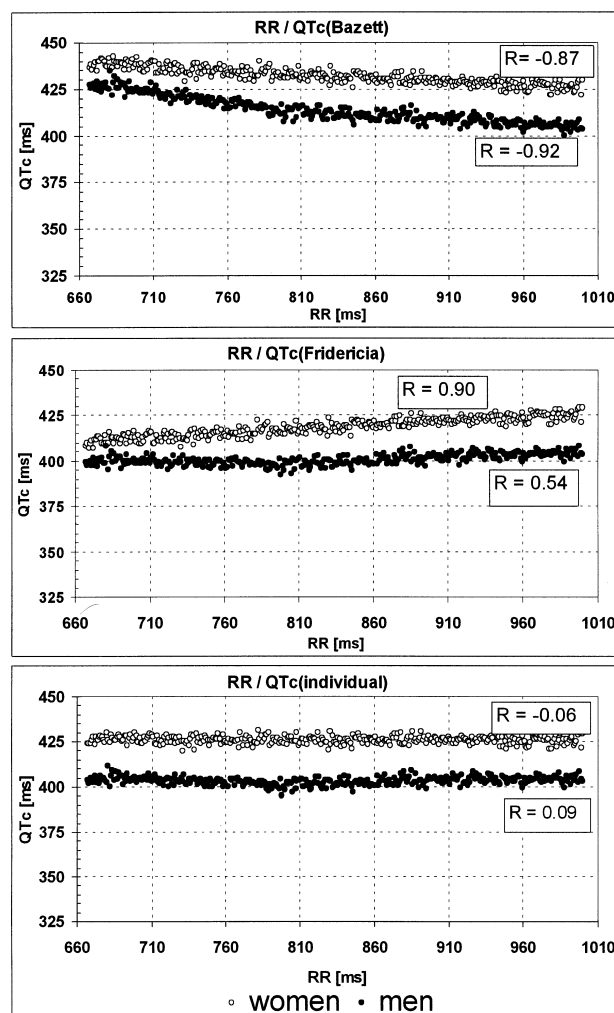


Figure 9. Correlation between the RR interval and QT interval corrected for heart rate with Bazett formula (top panel), Fridericia formula (middle panel) and individualized formulae (bottom panel). Pooled data from 24-hour ECG recordings in 24 healthy women (open circles) and 22 healthy men (closed circles). Only QT-RR data at heart rate of 60-90 b/min are presented. Note that even within this physiological range of resting heart rates, the QT interval corrected by Bazett formula (top panel) is strongly negatively correlated to the RR interval ($r = -0.92$ and -0.87 in men and women, respectively), rendering artificial QTc differences of about 20 ms. Although Fridericia formula (middle panel) renders better results in men, only the individualized QT correction formulae (bottom panel) produce QTc intervals that are practically heart rate-independent.

rection formulae, including the formulae of Bazett²⁸, Fridericia²⁹, Hodges³³, Sarma⁴², the Framingham study³², and others. Secondly, an optimized correction formula was derived by QT/RR regression modeling of the pooled drug-free data of all participants. Finally, individually optimized formulae were derived for each participant from the available 41 QT/RR data points obtained in the drug-free state. While the pooled drug-free regression found an optimized correction $QTc = QT/RR^{0.314}$, the correction coefficient α varied between 0.161 and 0.417 in individually optimized corrections $QTc = QT/RR^\alpha$.

While all the results with terfenadine confirmed previous findings that the drug prolongs QT interval⁴³⁻⁴⁵, the results with ebastine were hugely different with different previously published formulae and ranged from statistically significant prolongation to statistically sig-

nificant shortening of QTc. Moreover, the results obtained with previously published formulae were significantly dependent on the success of each formula to correct QT interval for heart rate (i.e. to provide QTc values that are heart rate-independent). The individually optimized heart rate correction formulae were superior to both the conventional heart rate correction formulae, as well as to the group optimized formula (the study showed that unlike terfenadine, ebastine does not prolong QTc interval). This study also suggested that the individual QT/RR relationship could be estimated from several tens of QT/RR data points.

These results also suggested that although inferior to the individualized heart rate correction approach, optimizing the heart rate correction formula for the pooled data of all subjects is superior to the application of any correction formula with fixed parameters. The regression analysis of the pooled QT-RR data therefore should be used only as an approximate heart rate correction approach when sufficient QT-RR data for each patient in drug-free state to estimate their individual QT/RR relationship are not available. Molnar et al.³⁷ also demonstrated the superiority of the individualized over the group-based approach for heart rate correction of the QT interval.

Similarly to drug studies, the application of arbitrarily chosen formula for heart rate correction of the QT interval in prospective studies assessing the prognostic value of the QTc interval should be discouraged. The practice of comparing the QTc interval in patient groups with different outcome without even reporting their heart rates seems unacceptable^{5,46}. Since estimation of the individual QT/RR relationship in such studies is usually not possible, a group-based heart rate correction approach should be applied^{14,47}. To the very least, the heart rate could be entered as an independent variable in addition to the QTc interval in multivariate regression analysis⁴⁸.

Conclusions

Time has proven the usefulness in everyday clinical practice of Bazett, Fridericia and other popular formulae for heart rate correction of the QT interval. In drug studies or other clinical investigations however, when higher precision of the measured QTc interval is required, this approach should be discouraged. In such cases, the application of individually optimized heart rate correction formulae should be adopted as a standard approach, especially when the drug or intervention change both the QT interval, as well as the heart rate. To derive individual heart rate correction formulae, it is crucial to obtain a sufficient number of ECGs in each subject over a significant physiological range of heart rates.

References

1. Schwartz PJ, Wolf S. QT interval prolongation as predictor of sudden death in patients with myocardial infarction. *Circulation* 1978; 57: 1074-7.

2. Karjalainen J, Reunanen A, Ristola P, Viitasalo M. QT interval as a cardiac risk factor in a middle-aged population. *Heart* 1997; 77: 543-8.
3. Elming H, Holm E, Jun L, et al. The prognostic value of the QT interval and QT interval dispersion in all-cause and cardiac mortality in a population of Danish citizens. *Eur Heart J* 1998; 19: 1391-400.
4. De Bruyne MC, Hoes AW, Kors JA, Hofman A, van Bommel JH, Grobbee DE. Prolonged QT interval predicts cardiac and all-cause mortality in the elderly. The Rotterdam Study. *Eur Heart J* 1999; 20: 278-84.
5. Okin PM, Devereux RB, Howard BV, Fabsitz RR, Lee ET, Welty TK. Assessment of QT interval and QT dispersion for prediction of all-cause and cardiovascular mortality in American Indians. The Strong Heart Study. *Circulation* 2000; 101: 61-6.
6. Report on a policy conference of the European Society of Cardiology. The potential for QT prolongation and proarrhythmia by non-antiarrhythmic drugs: clinical and regulatory implications. *Eur Heart J* 2000; 21: 1216-31.
7. Priori SG, Napolitano C, Schwartz PJ. Low penetrance in the long QT syndrome. Clinical impact. *Circulation* 1999; 99: 529-33.
8. Roden DM. The genetics of the long QT syndrome. *ACC Current Journal Review* 2002; 11: 70-3.
9. Walker AM, Sznke P, Weatherby LB, et al. The risk of serious cardiac arrhythmias among cisapride users in the United Kingdom and Canada. *Am J Med* 1999; 107: 356-62.
10. Waller AD. A demonstration on man of electromotive changes accompanying the heart's beat. *J Physiol* 1887; 8: 229-35.
11. Thurston E. The length of the systole of the heart, as estimated from sphygmographic tracings. *J Anat Physiol* 1876; 10: 494-501.
12. Garrod AH. On cardiograph tracings from the human chest-wall. *J Anat Physiol* 1871; 5: 2-27.
13. Garrod AH. *Proc Royal Soc Lond* 1870: 351.
14. Malik M. Problems of heart rate correction in assessment of drug-induced QT interval prolongation. *J Cardiovasc Electrophysiol* 2001; 12: 411-20.
15. Ljung O. A simple formula for clinical interpretation of the QT interval data. *Acta Med Scand* 1949; 134: 79-86.
16. Hodges M. (1997) Rate Correction of the QT Interval. *Cardiac Electrophysiol Rev* 3:360-363.
17. Rautaharju PM, Warren JW, Calhoun HP. Estimation of QT prolongation. A persistent, avoidable error in computer electrocardiography. *J Electrocardiol* 1990; 23 (Suppl): 111-7.
18. Funck-Brentano K, Jaillon P. Rate-corrected QT interval: techniques and limitations. *Am J Cardiol* 1993; 72: 17B-22B.
19. Aytemir K, Maarouf N, Gallagher MM, Yap YG, Waktare JE, Malik M. Comparison of formulae for heart rate correction of QT interval in exercise electrocardiograms. *Pacing Clin Electrophysiol* 1999; 22: 1397-401.
20. Malik M. The imprecision in heart rate correction may lead to artificial observations of drug-induced QT interval changes. *Pacing Clin Electrophysiol* 2002; 25: 209-16.
21. Rickards AF, Norman J. Relation between QT interval and heart rate. New design of physiologically adaptive cardiac pacemaker. *Br Heart J* 1981; 45: 56-61.
22. Browne KF, Prystowsky E, Heger JJ, Zipes DP. Modulation of the Q-T interval by the autonomic nervous system. *Pacing Clin Electrophysiol* 1983; 6: 1050-6.
23. Cappato R, Alboni P, Pedroni P, Gilli G, Antonioli GE. Sympathetic and vagal influences on rate-dependent changes of QT interval in healthy subjects. *Am J Cardiol* 1991; 68: 1188-93.
24. Lau CP, Freedman AR, Fleming S, Malik M, Camm AJ, Ward DE. Hysteresis of the ventricular paced QT interval in response to abrupt changes in pacing rate. *Cardiovasc Res* 1988; 22: 67-72.
25. Franz MR, Swerdlow CD, Liem LB, Schaefer J. Cycle length dependence of human action potential duration in vivo: effects of single extrastimuli, sudden sustained rate acceleration and deceleration, and different steady-state frequencies. *J Clin Invest* 1988; 82: 972-9.
26. Kawataki M, Kashima T, Toda H, Tanaka H. Relation between QT interval and heart rate. Applications and limitations of Bazett's formula. *J Electrocardiol* 1984; 17: 371-5.
27. Mayeda I. On time relation between systolic duration of heart and pulse rate. *Acta Scholae Med Univ Imp Kioto* 1934; 17: 53-5.
28. Bazett HC. An analysis of the time-relations of electrocardiograms. *Heart* 1920; 7: 353-70.
29. Fridericia LS. Die Systolendauer im Elektrokardiogramm bei normalen Menschen und bei Herzkranken. *Acta Med Scand* 1920; 53: 469-86.
30. Larsen K, Skulason T. Det normale Elektrokardiogram. I. Analyse af Ekstremitetsafledningerne hos 100 sunde Mennesker I Alderen fra 30 til 50 Aar. *Nord Med* 1941; 9: 350-8.
31. Schlamowitz I. An analysis of the time relationships within the cardiac cycle in electrocardiograms of normal men. I. The duration of the Q-T interval and its relationship to the cycle length (R-R interval). *Am Heart J* 1946; 31: 329-42.
32. Sagie A, Larson MG, Goldberg RJ, Bengtson JR, Levy D. An improved method for adjusting the QT interval for heart rate (the Framingham study). *Am J Cardiol* 1992; 70: 797-801.
33. Hodges M, Salerno D, Erlén D. Bazett's QT correction reviewed: evidence that a linear QT Correction for heart rate is better. (abstr) *J Am Coll Cardiol* 1983; 1: 694.
34. Karjalainen J, Viitasalo M, Manttari M, Manninen V. Relation between QT intervals and heart rates from 40 to 120 beats/min in rest electrocardiograms of men and a simple method to adjust QT interval values. *J Am Coll Cardiol* 1994; 23: 1547-53.
35. Wohlfart B, Pahlm O. Normal values for QT interval in ECG during ramp exercise on bicycle. *Clin Physiol* 1994; 14: 371-7.
36. Davey P. A new physiological method for heart rate correction of the QT interval. *Heart* 1999; 82: 183-6.
37. Molnar J, Weiss J, Zhang F, Rosenthal JE. Evaluation of five QT correction formulas using a software assisted method of continuous QT measurement from 24-hour Holter recordings. *Am J Cardiol* 1996; 78: 920-6.
38. Malik M, Färbom P, Batchvarov V, Hnatkova K, Camm AJ. Relation between QT and RR intervals is highly individual among healthy subjects: implications for heart rate correction of the QT interval. *Heart* 2002; 87: 220-8.
39. Lecocq B, Lecocq V, Jaillon P. Physiologic relation between cardiac cycle and QT duration in healthy volunteers. *Am J Cardiol* 1989; 63: 481-6.
40. Batchvarov VN, Ghuran A, Smetana P, et al. QT-RR relationship in healthy subjects exhibits substantial intersubject variability and high intrasubject stability. *Am J Physiol* 2002; 282: H2356-H2363.
41. Batchvarov VN, Smetana P, Ghuran A, Hnatkova K, Camm AJ, Malik M. Comparison of Bazett, Fridericia, and an individually derived formula for heart rate correction of the QT interval. (abstr) *Pacing Clin Electrophysiol* 2002; 24 (Part II): 606.
42. Sarma JS, Sarma RJ, Bilitch M, Katz D, Song SL. An exponential formula for heart rate dependence of QT interval during exercise and cardiac pacing in humans: reevaluation of Bazett's formula. *Am J Cardiol* 1984; 54: 103-8.
43. Honig PK, Wortham DC, Zamani K, Conner DP, Mullin JC, Cantilena LR. Terfenadine-ketoconazole interaction: phar-

- macokinetic and electrocardiographic consequences. *JAMA* 1993; 269: 1513-8.
44. Benton RE, Honig PK, Zamani K, Cantilena LR, Woosley RL. Grapefruit juice alters terfenadine pharmacokinetics, resulting in prolongation of repolarization on the electrocardiogram. *Clin Pharmacol Ther* 1996; 59: 383-8.
45. Clifford CP, Adams DA, Murray S, et al. The cardiac effects of terfenadine after inhibition of its metabolism by grapefruit juice. *Eur J Clin Pharmacol* 1997; 52: 311-5.
46. Wong KY, Mac Walter RS, Douglas D, Fraser HW, Ogston SA, Struthers AD. Long QTc predicts future cardiac death in stroke survivors. *Heart* 2003; 89: 377-81.
47. Fauchier L, Maison-Blanche P, Forhan A, et al, and the DESIR Study Group. Association between heart rate-corrected QT interval and coronary risk factors in 2894 healthy subjects (the DESIR study). *Am J Cardiol* 2000; 86: 557-9.
48. Brendorp B, Elming H, Jun L, et al, for the DIAMOND Study Group. QTc interval as a guide to select those patients with congestive heart failure and reduced left ventricular systolic function who will benefit from antiarrhythmic treatment with dofetilide. *Circulation* 2001; 103: 1422-7.

PROGNOSTIC VALUE OF THE T WAVE COMPLEXITY

Luigi De Ambroggi, Alexandru D. Corlan

Department of Cardiology, Istituto Policlinico San Donato, San Donato Milanese (MI), Italy

The T wave complexity can be studied using multiple thoracic leads (surface potential maps) or the 12-lead ECG. Body surface potential maps (BSPM) have two major advantages over the conventional 12 leads: to explore the entire chest surface and to be more sensitive in detecting local electrical events. On the other hand, the method of BSPM is impractical for wide clinical use. Different methods of analysis of BSPM have been used to study repolarization potentials: instantaneous potential distribution, QRS-T integral maps, eigenvector analysis, principal component analysis, autocorrelation analysis. By means of the conventional 12-lead ECG, different variables for quantitation of repolarization heterogeneity have been proposed, in addition to QT dispersion, that has been proved to be a gross estimate of repolarization abnormalities: principal components, total cosine R-to-T, T wave residuum and others. These variables showed good prognostic value in large clinical trials recently reported.

Introduction

Experimental studies on wedge preparations have clearly demonstrated that different patterns of the ECG T-U waves depend on the characteristics of action potential in different myocardial strata and, specifically, on variations of the "physiological" transmural dispersion of repolarization¹.

Many investigations have focused on the key role of ventricular repolarization abnormalities in the genesis of cardiac arrhythmias. Schematically, vulnerability to

arrhythmias can arise from two conditions of repolarization process: 1) a state of heterogeneity of repolarization, i.e. a greater than normal dispersion of recovery times, and 2) a dynamic (beat-to-beat) variation of repolarization sequence. This last condition, which frequently occurs in ischemic situations, can be detected by different methods (e.g., analysis of T wave alternans, RR/QT relationship variations). The first condition can be detected by analyzing a single beat, using the 12-lead ECG or multiple thoracic leads, that is body surface potential maps (BSPM).

Body surface potential maps

BSPM have two major advantages over the conventional 12-lead ECG: 1) to explore the entire chest surface (in fact, BSPM is the only method that provides all the information on the cardiac electric field available at the body surface); 2) to be more sensitive in detecting local electrical events, such as local conduction disturbances or regional heterogeneities of ventricular recovery. On the other hand, the method of BSPM is impractical for wide clinical use.

Maps can be recorded with different lead system and various methods of analysis of BSPM have been used to study repolarization potentials.

Instantaneous potential maps. In normal subjects the potential distribution throughout the ventricular repolarization is usually bipolar, with limited shift of the potential maximum and minimum on the thorax. In some pathological conditions the locations of the potential maximum and minimum can be different than in normal subjects and sometimes, as in myocardial ischemia, a multipolar distribution could be observed during some portions of repolarization². This multipolar pattern reflects the complexity of the cardiac generator during that time interval, i.e. the simultaneous presence of multiple regions at quite different potential levels. This situation can favor the reentry phenomenon and thus the initiation of ventricular arrhythmias.

QRS-T integral maps. Areas of QRS-T deflections mainly reflect the intrinsic repolarization properties and are largely independent of ventricular excitation sequence. A complex, multipolar pattern has been related, on the basis of experimental observations, to local heterogeneities of the ventricular recovery process and thus to cardiac states of vulnerability to arrhythmias³. In our experience, a clear multipolar pattern is visible only in a small percentage of patients affected by ventricular arrhythmias. A multipolar distribution most likely reflects only gross regional inequalities of repolarization, and may not represent a marker sufficiently sensitive for minor disparities.

Eigenvector analysis. In 1981 Lux et al.⁴ proposed a method by which each potential map could be repre-

sented as a weighted sum of a limited number of fundamental patterns (eigenvectors) common to both control subjects and patients. This method makes it possible the detection and quantitation of nondipolar components not evident on visual inspection of the integral maps. In fact, the first three eigenvectors, displayed as eigenvector contour maps, generally show a smooth dipolar distribution with different locations of the peak values, whereas the eigenvectors beyond the third have a multipolar distribution. Thus, the cumulative contribution of the eigenvectors beyond the third to an individual map, expressed as percentage contribution of the total map content, has been considered the “non-dipolar content” of that map. According to this method, we calculated the non-dipolar content of QRS-T integral maps in different groups of patients (long QT syndrome, old myocardial infarction with and without episodes of sustained ventricular tachycardia) and in a control group of healthy subjects^{5,6}. On average, the non-dipolar content was significantly lower in controls than in long QT syndrome patients or in patients with myocardial infarction and ventricular tachycardia.

Principal component analysis. We applied principal component analysis to all ST-T waves recorded on the thoracic surface. Principal component analysis allows the identification of one set of values, corresponding to the first principal component, which better represents most of the original sets of data recorded. Usually the first three components provide nearly the total variation of the original data.

We proposed to compute the similarity index (ratio of first eigenvalue by the sum of all eigenvalues). The value of similarity index is inversely proportional to the variability of T wave morphologies and a low value is considered a marker of repolarization heterogeneity. In our experience, similarity index was found significantly lower than normal in patients affected by congenital long QT syndrome⁷, in patients with arrhythmogenic right ventricular dysplasia and ventricular tachycardias⁸, and in patients with myocardial infarction.

Other repolarization variables (autocorrelation analysis). In order to analyzing the instantaneous variations of repolarization potentials we proposed two indices: early repolarization deviation index (ERDI) and late repolarization deviation index (LRDI). Visually, the pattern of potential maps is generally constant during normal repolarization, apart from changes in amplitude. The ERDI and LRDI are numerical indices which describe deviations from this behavior during repolarization, from the J point to the T peak and from the peak to the end of T wave, respectively^{9,10}. We computed these indices in small series of patients with different cardiac diseases (arrhythmogenic right ventricular dysplasia, left ventricular hypertrophy due to aortic stenosis, myocardial infarction with and without arrhythmias), and in some groups significant differences from normal subjects were found.

Conventional twelve-lead electrocardiogram

In recent years various methods for quantitation of repolarization heterogeneity from the standard 12-lead ECG have been proposed.

QT dispersion. The measurement of 12-lead QT interval dispersion was widely used as an index of repolarization heterogeneity mainly because of its simplicity, but it has several limitations. The major limitation is that this measure cannot be related to the “true” spatial heterogeneity of repolarization, since each surface lead is influenced by the electrical activity of the entire heart. Moreover there are other well-known methodological limitations (e.g., accuracy of measurements, inter-intraobserver variability, number of leads used) which can partly explain the controversial results reported in the literature¹¹. In summary, whereas initial results coming from small retrospective studies seemed to prove the prognostic value of QT dispersion as a risk stratifier, more recent prospective trials did not confirm these data^{12,13}. Actually, QT dispersion can be considered only a gross estimate of repolarization abnormalities.

Principal component analysis. Principal component analysis has been applied also for analysis of the 12-lead ECG waveforms. Generally, as for BSPM, the method defines several independent components, that contain all the information of the T waves of the 12-lead ECG. Recently Okin et al.¹⁴ reported that an increased principal component analysis ratio was an independent predictor of cardiovascular mortality in a large population of American Indians.

T wave morphology descriptors. In order to identify more precise descriptors of the 12-lead T wave morphology a set of new variables has been proposed¹⁵, that measure the spatial and temporal variations of T wave morphology, the difference of the mean wavefront direction between ventricular depolarization and repolarization, the non-dipolar component. These variables have the advantage to be not critically dependent on time-domain measurements (as the identification of the T wave end) and showed good reproducibility.

The prognostic value of the total cosine R-to-T, an estimate of the angle between repolarization and depolarization wavefront, and the T wave loop dispersion were found significantly associated with clinical events in 261 post-myocardial infarction patients¹⁶.

Recently, an abnormal spatial QRS-T angle showed a strong predictive value for cardiac mortality in a general population > 55 years of the Rotterdam Study¹⁷.

Another descriptor, the T wave residuum, that is an index of non-dipolar content of the 12-lead ECG, was found to predict mortality in 772 US veterans with cardiovascular diseases followed-up for 10.4 ± 3.8 years¹⁸. On univariate analysis, patients with T wave residua above the median value had significant worse survival compared to patients with values below the median.

Conclusion

The complexity of the surface T waves reflects complexity of the repolarization process in the heart, which in turn plays a role in arrhythmogenesis. Several variables can describe T wave complexity with different degrees of accuracy. Nevertheless, the pathophysiological meaning of each descriptor, that characterizes the complexity, has still to be clarified by experimental and modeling studies.

References

1. Yan GX, Antzelevitch C. Cellular basis for the normal T wave and the electrocardiographic manifestations of the long QT syndrome. *Circulation* 1998; 98: 1928-36.
2. De Ambroggi L, Musso E, Taccardi B. Body surface mapping. In: Macfarlane PW, Lawrie TD, eds. *Comprehensive electrocardiology. Theory and practice in health and disease*. Vol II. Oxford: Pergamon Press, 1989; 27: 1015-49.
3. Urie PM, Burgess MJ, Lux RL, Wyatt RF, Abildskov JA. The electrocardiographic recognition of cardiac states at high risk of ventricular arrhythmias. *Circ Res* 1978; 42: 350-8.
4. Lux RL, Evans AK, Burgess MJ, Wyatt RF, Abildskov JA. Redundancy reduction for improved display and analysis of body surface potential maps. I. Spatial compression. *Circ Res* 1981; 49: 186-96.
5. De Ambroggi L, Bertoni T, Locati E, Stramba-Badiale M, Schwartz PJ. Mapping of body surface potentials in patients with the idiopathic long QT syndrome. *Circulation* 1986; 74: 1334-45.
6. Bertoni T, Breggi ML, Marconi M, Bonifaccio G, De Ambroggi L. Usefulness of the integral maps to detect vulnerability to malignant arrhythmias in patients with old myocardial infarction. In: Schubert E, ed. *Electrocardiology '87*. Berlin: Akademie-Verlag, 1988: 247-50.
7. De Ambroggi L, Negroni MS, Monza E, Bertoni T, Schwartz PJ. Dispersion of ventricular repolarization in the long QT syndrome. *Am J Cardiol* 1991; 68: 614-20.
8. De Ambroggi L, Aimè E, Ceriotti C, Rovida M, Negroni S. Mapping of ventricular repolarization potentials in patients with arrhythmogenic right ventricular dysplasia. Principal component analysis of the ST-T waves. *Circulation* 1997; 96: 4314-8.
9. Corlan AD, De Ambroggi L. New quantitative methods of ventricular repolarization analysis in patients with left ventricular hypertrophy. *Ital Heart J* 2000; 1: 542-8.
10. Corlan AD, Macfarlane PW, De Ambroggi L. Gender differences in stability of the instantaneous patterns of body surface potentials during ventricular repolarisation. *Med Biol Eng Comput* 2003; 41: 536-42.
11. Malik M. QT dispersion: time for an obituary? *Eur Heart J* 2000; 21: 955-7.
12. Zabel M, Klingenheden T, Franz MR, Hohnloser S. Assessment of QT dispersion for prediction of mortality or arrhythmic events after myocardial infarction. Results of a prospective, long-term follow-up study. *Circulation* 1998; 97: 2543-50.
13. Brendorp B, Elming H, Jun L, et al. QT dispersion has no prognostic information for patients with advanced congestive heart failure and reduced left ventricular systolic function. *Circulation* 2001; 103: 831-5.
14. Okin PM, Devereux RB, Fabsitz RR, et al. Principal component analysis of the T wave and prediction of cardiovas-

cular mortality in American Indians. The Strong Heart Study. *Circulation* 2002; 105: 714-9.

15. Acar B, Yi G, Hnatkova K, et al. Spatial, temporal and wave-front direction characteristics of 12-lead T wave morphology. *Med Biol Eng Comput* 1999; 37: 574-84.
16. Zabel M, Acar B, Klingenheden T, et al. Analysis of T wave morphology for risk stratification after myocardial infarction. *Circulation* 2000; 102: 1252-7.
17. Kardys I, Kors JA, van der Meer IM, et al. Spatial QRS-T angle predicts cardiac death in a general population. *Eur Heart J* 2003; 24: 1357-64.
18. Zabel M, Malik M, Hnatkova K, et al. Analysis of T wave morphology from the 12-lead electrocardiogram for prediction of long-term prognosis in male US veterans. *Circulation* 2002; 105: 1066-70.

FREQUENCY-DOMAIN ANALYSIS OF LEFT VENTRICULAR HYPERTROPHY BY CEREBROCARDIOGRAM IS AN ACCURATE NEW TOOL

Paolo Emilio Puddu, Michele Schiariti, Giuseppe Massimo Ciavarella*, Domenico Cuturello, Maddalena Colicci, Coskun Usta, Dan Q. Fang

*Institute of Heart and Great Vessels "Attilio Reale", *Clinical Pathophysiology, "La Sapienza" University, Rome, Italy*

Objective. Time-domain analysis of electrical vectors recorded by standard electrocardiogram (ECG) identifies left ventricular hypertrophy (LVH) with poor sensitivity. Although time-voltage integral increases of the summed left ventricular dipole have a higher pre-test probability to perform better than changes in voltage (Sokolow-Lyon index or 12-lead QRS sum) or QRS duration alone, relatively new indexes of LVH such as Cornell product also showed sub-maximal accuracy.

Measurements. Cerebro-electrocardiography (from the Latin term *crebr* = frequency) is the first clinical application of the most recent bio-cybernetic theories whereby the heart is considered as the process-controller and great vessels, blood and electrical conduction are the transmission system. Quantum dynamics, the core technology, is used to record and analyze cardiac electrophysiological signals in the frequency domain (up to 25 Hz). Cerebrocardiogram (CCG) is obtained non-invasively (in 88 s) and provides cardiac energetic spectrum based on a series of harmonics, the first representing heart rate. We concentrate here on the 1 to 8 Hz spectrum and the sum of the initial 4 peaks (4P sum, mW) as indexes of LVH.

Results. We compared ECG time-domain to CCG frequency-domain (4P sum in each of 12 standard ECG leads) indexes in 22 subjects (67% men, mean age 57 ± 15 years): 7 of these had an echocardiographic mass index (Devereux, MID) of $> 145 \text{ g/m}^2$, so defined as reference LVH. MID was treated as a continuous variable ($118 \pm 32 \text{ g/m}^2$) and both linear ($Y[\text{MID}] = a + bx$) and curvilinear ($Y[\text{MID}] = a + b \ln x/x$) fits were obtained, x values being either ECG or CCG (repeatability $\pm 5\%$) predictors. LVH diagnostic accuracy (based on the literature cut-offs) was also ascertained. Sokolow-Lyon index, either linearly ($r^2 = 0.064$, $F = 1.381$) or curvilinearly ($r^2 = 0.033$, $F = 0.675$) showed a poor fit with MID and the predictive accuracy was 68%. Both 12-lead QRS sum and Cornell

product had a fairly good predictive accuracy (86 and 77%, respectively), yet linear ($r^2 = 0.259$, $F = 7.001$ and $r^2 = 0.219$, $F = 5.614$, respectively) and curvilinear ($r^2 = 0.218$, $F = 5.569$ and $r^2 = 0.268$, $F = 7.339$, respectively) fits were poor. On the other hand, CCG 4P sum showed both the best fit with MID (linear $r^2 = 0.323$, $F = 9.550$ and curvilinear $r^2 = 0.640$, $F = 35.578$) and a good predictive accuracy (86%).

Conclusions. Frequency-domain CCG may index LVH with a high accuracy and the prediction of MID is largely superior (based on F statistics) to standard time-domain ECG parameters, either taking voltage alone or time-voltage integral into consideration. CCG may thus be a new tool to help indexing the probabilistic presentation of LVH.

Cardiac electrical activity is recorded in time domain by classic electrocardiography (ECG) since Einthoven's invention of the string galvanometer in 1903. Later, a series of applications has contributed to significantly enlarge the clinical usefulness of time-domain ECG: they spanned from vectorcardiography to magnetocardiography and stress ECG, from 24-hour continuous ambulatory monitoring to signal averaged ECG and to ventricular late potential investigations, body surface mapping of ECG and heart rate variability studies¹. Review of all these techniques is well beyond our scope: suffice to say, however, that their diagnostic accuracy is not perfect and in some instances unfair, to the extent that efforts to increase it are worthwhile.

Frequency-domain analysis of electrical vectors is a relatively new technique²⁻⁹. The basic concept is derived from physics: here energy wave length (frequency) is used to define the spectrum of a radiant (or incandescent) source. Thus the frequency spectrum provides means to interpret the type of energy involved in the entire range (from 0 to 10^{23} cycles/s) of those present in the universe, from cosmic photons to ultraviolet radiations, from visible light to radio waves, from heat to electrical currents. The electrophysiological signals generated by the heart are a peculiar type of energy and may therefore be treated applying concepts of frequency-domain analysis and their mathematical notations and derivations⁵.

Under the names of ECG multiphase information technology or cardiac ultra-phase information diagnosis (CUPID)^{2,5,7,9} or different technologies^{3,4,6,8} important clinical diagnostic capabilities of frequency-domain analysis of ECG have been reported so far in a variety of cardiac abnormalities with excellent diagnostic accuracy, especially in coronary artery disease and left ventricular hypertrophy (LVH)^{3,4,7-9}. The basic principles of frequency-domain analysis have also been applied external to electrophysiological or strictly to cardiac areas for diagnostic purposes¹⁰⁻¹⁴. More recently named crebro-electrocardiography (CCG: from the Latin term *crebr*, theoretical idea of frequency) multiphase technology uses bio-cybernetic theories whereby the heart is considered as the engine (pump or process-controller) and the great vessels, the blood and the electrical conduction are the transmission system and quantum electrodynamics to both record and analyze cardiac electrophysiological sig-

nals. CCG provides cardiac energetic spectrum which may be defined based on a series of harmonics, the first representing heart rate. Fast Fourier transformation (obtained from the 12 conventional ECG leads) gives cardiac power spectrum along with peculiar parameters such as impulse response, coherence and cross-correlation (using ECG leads D_2 and V_5). The morphology of all these parameters is used to define intrinsic characteristics of the cardiovascular system. A complex mathematical analysis enables to derive functions describing cardiac properties interpreted bio-cybernetically. These functions are then used to index myocardial contractility, electrical conduction, and coronary flow. All of these characteristics have been recently reviewed⁵ and we therefore skip several details in the present study.

We report here an experience with CCG in the area of LVH comparing data with those of three indexes proposed from time-domain ECG, of which the Cornell index seemed to be a particularly useful one¹⁵⁻¹⁹. Correlations with left ventricular mass index derived from echocardiography (Devereux, MID)^{20,21} are compared using both linear and non-linear methods. It is concluded that frequency-domain CCG may index LVH with a high accuracy and the prediction of MID is largely superior to standard time-domain ECG parameters. CCG may thus be a new tool to help indexing the probabilistic presentation of LVH.

Methods and results

The technique that we named crebro-electrocardiography is the first clinical application of the most recent bio-cybernetic theories whereby the heart is considered as the process-controller and great vessels, blood and electrical conduction are the transmission system. Using quantum dynamics electrophysiological signals are recorded and analyzed in frequency domain (up to 25 Hz). Under the previous name of CUPID the technique has been extensively reviewed and received Food and Drug Administration approval for non-invasive cardiac testing, after reviewing 2848 cases from the original correlative studies⁵. Briefly, CCG is obtained non-invasively (in 88 s) and provides cardiac energetic (or power) spectrum based on a series of harmonics, the first representing heart rate. A complex mathematical formulation⁵ is used to obtain the power spectrum (Fig. 1), mainly based on fast Fourier transformation. We concentrate here on the 1 to 8 Hz spectrum and the sum of the initial 4 peaks (4P sum, mW) as indexes of LVH (Fig. 2). These parameters have been previously recognized as sensitive indexes of LVH^{5,9}.

We compared ECG time-domain to CCG frequency-domain (4P sum in each of 12 standard ECG leads) indexes in 22 subjects (67% men, mean age 57 ± 15 years): 7 of these had a MID of $> 145 \text{ g/m}^2$, so defined, with slight modification compared to the reference standard of $> 125 \text{ g/m}^2$ ^{20,21}, our reference LVH. The study subjects were selected among hypertensive patients in

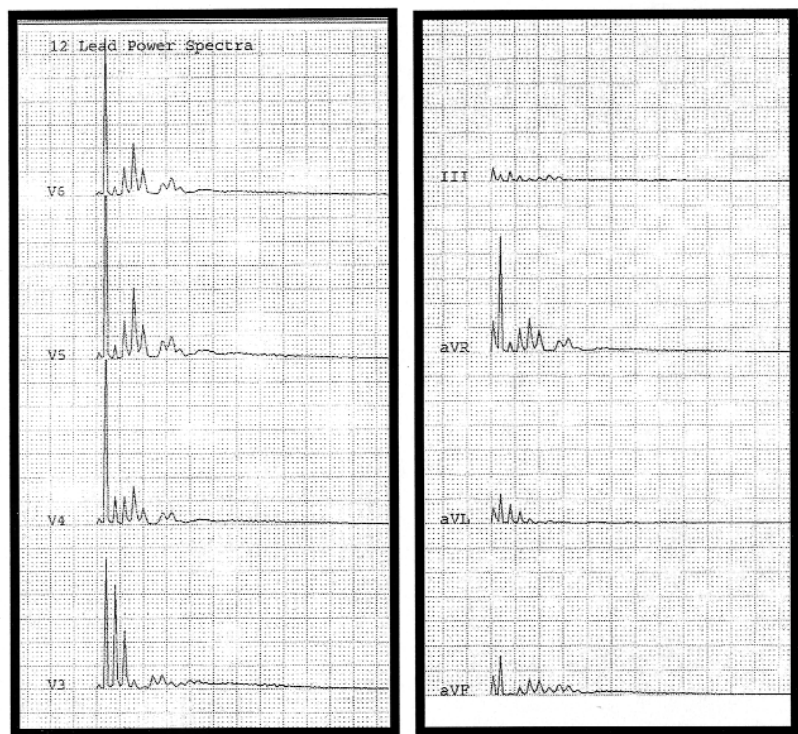


Figure 1. Crebrocardiographic power spectra of leads V₃-V₆ (left panel: reduced 40%) and D₃, aVR, aVL, aVF (right panel: reduced 40%) in a subject with normal left ventricular mass index (93.6 g/m²).

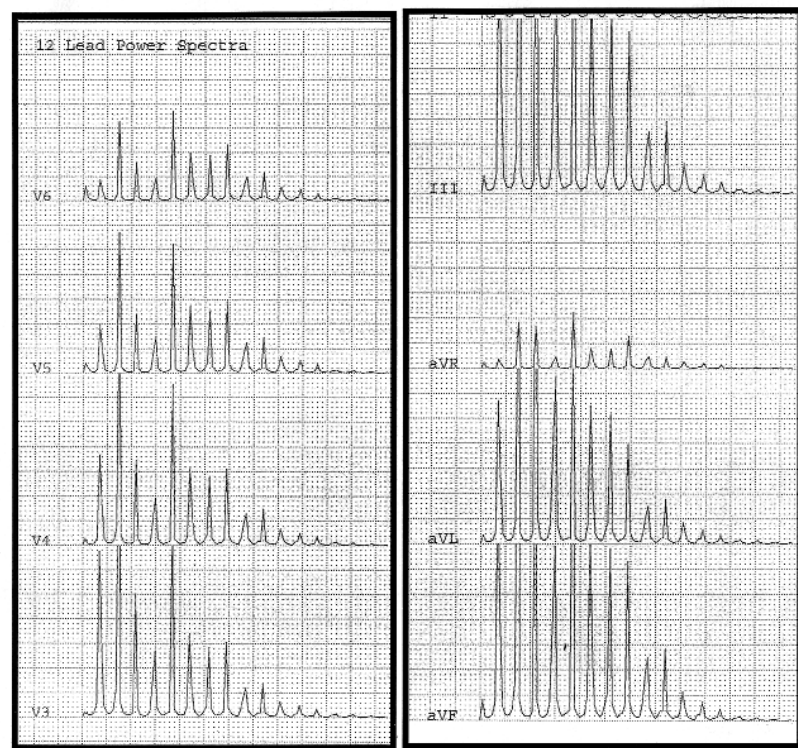


Figure 2. Crebrocardiographic power spectra of leads V₃-V₆ (left panel reduced 40%) and D₃, aVR, aVL, aVF (right panel reduced 40%) in a subject with left ventricular hypertrophy and a highly increased left ventricular mass index (152.3 g/m²). Note that power spectra of V₃, D₃, aVL and aVF present the initial 4 peak values extremely increased as compared to power spectra of figure 1. In particular, note the large difference in aVL.

pharmacological treatment (n = 10) and there were 12 controls without treatment. Details of the study have been reported previously⁹. There was no difference between LVH group and controls in either mean age (69 ± 10 and

52 ± 13 years, respectively) or sex distribution (57 and 67% men, respectively). MID was treated as a continuous variable for the overall 22 subjects (118 ± 32 g/m²) and both linear (Y[MID] = a+bx) and curvilinear

($Y[MID] = a + b \ln x/x$) fits were obtained, x values being either ECG (three indexes selected: Sokolow-Lyon¹⁵, 12-lead QRS sum¹⁶ and Cornell product¹⁷⁻¹⁹) or CCG (repeatability $\pm 5\%$) predictors. LVH diagnostic accuracy [based on the literature cut-offs, 3.4 mV¹⁵, 18.6 mV¹⁶ and 2440 mm*ms, respectively (having 10 mm = 1 mV)¹⁷⁻¹⁹] was also ascertained.

Sokolow-Lyon index, either linearly ($r^2 = 0.064$, $F = 1.381$) or curvilinearly ($r^2 = 0.033$, $F = 0.675$) showed a poor fit with MID and the predictive accuracy was 68%. Both 12-lead QRS sum and Cornell product had a fairly good predictive accuracy (86 and 77%, respectively), yet linear ($r^2 = 0.259$, $F = 7.001$ and $r^2 = 0.219$, $F = 5.614$, respectively) (Fig. 3) and curvilinear ($r^2 = 0.218$, $F = 5.569$ and $r^2 = 0.268$, $F = 7.339$, respectively) (Fig. 4) fits were poor. On the other hand, CCG 4P

sum showed both the best fit with MID [linear $r^2 = 0.323$, $F = 9.550$ (Fig. 5), and curvilinear $r^2 = 0.640$, $F = 35.578$ (Fig. 6)] and a good predictive accuracy (86%). Noteworthy, leads aVL and V_3 provided the best fit results, based on multivariate analysis, as compared to data obtained in all 12 standard leads⁹. Although 4P sum measured in aVL showed the best fit in comparison with time-domain indexes of LVH, similar excellent fits and accuracy were obtained in V_3 (data not shown).

Discussion

Time-domain analysis of electrical vectors recorded by standard ECG identifies LVH with poor sensitivity. Although time-voltage integral increases of the summed

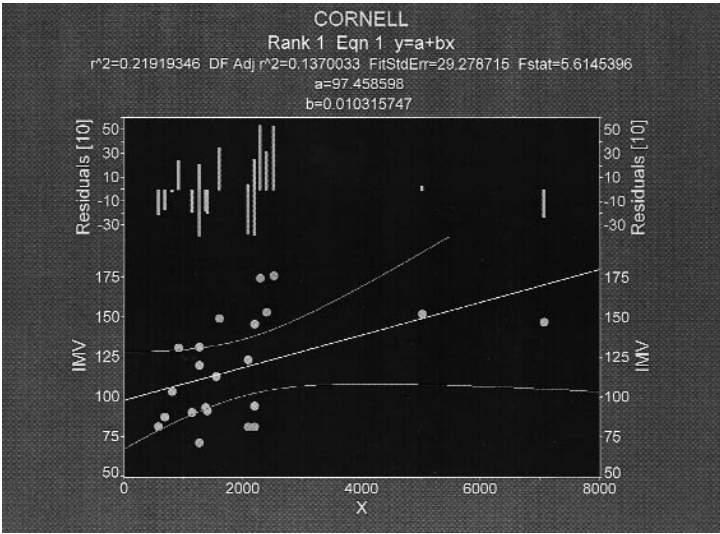


Figure 3. Linear correlation between Cornell product¹⁷⁻¹⁹ and left ventricular mass index (IMV) in the overall sample study ($n = 22$). The graph shows correlation line with 95% confidence intervals and residuals. All correlation parameters are also illustrated. There are seven data points outside acceptable residual range. Points ($n = 2$) with Cornell product above normal limits (2440 mm*ms) are in 95% confidence limits.

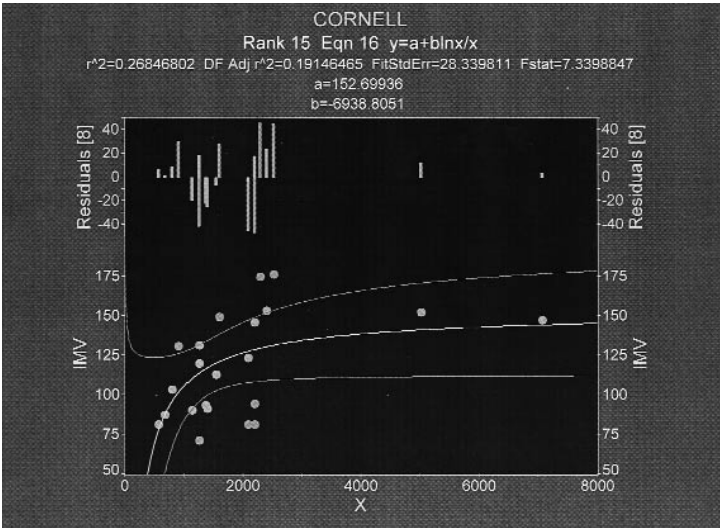


Figure 4. Curvilinear correlation between Cornell product¹⁷⁻¹⁹ and left ventricular mass index (IMV) in the overall sample study ($n = 22$). The graph shows correlation line with 95% confidence intervals and residuals. All correlation parameters are also illustrated. There are 8 data points outside acceptable residual range. Points ($n = 2$) with Cornell product above normal limits (2440 mm*ms) are in 95% confidence limits.

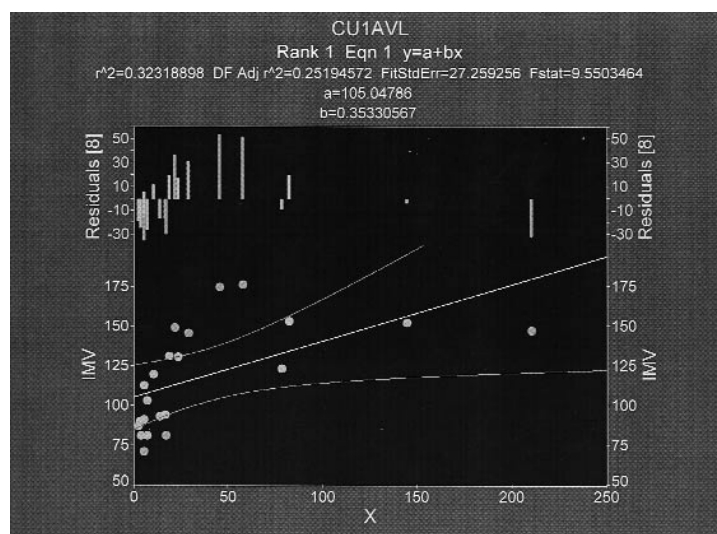


Figure 5. Linear correlation between crebrocardiographic sum of the initial 4 peaks in aVL (CU1AVL)⁹ and left ventricular mass index (IMV) in the overall sample study (n = 22). The graph shows correlation line with 95% confidence intervals and residuals. All correlation parameters are also illustrated. There are 7 data points outside acceptable residual range. There are 4 of 6 points with the crebrocardiographic index above normal limits (45 mm) which are in 95% confidence limits.

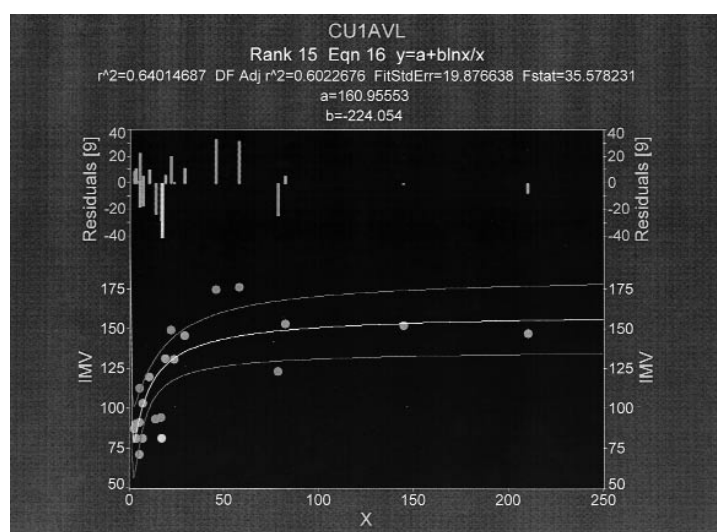


Figure 6. Curvilinear correlation between crebrocardiographic sum of the initial 4 peaks in aVL (CU1AVL)⁹ and left ventricular mass index (IMV) in the overall sample study (n = 22). The graph shows correlation line with 95% confidence intervals and residuals. All correlation parameters are also illustrated. There are 7 data points outside acceptable residual range. There are 3 of 6 points with the crebrocardiographic index above normal limits (45 mm) which are in 95% confidence limits. However, as compared to figure 5, residuals are shorter.

left ventricular dipole have a higher pre-test probability to perform better than changes in voltage (Sokolow-Lyon index or 12-lead QRS sum) or QRS duration alone, relatively new indexes of LVH such as Cornell product also showed submaximal accuracy¹⁵⁻²¹.

CCG comes some 100 years after ECG was first proposed and represents a further development to tune clinical diagnosis by analysis of cardiac electrophysiological signals⁵. Sophisticated, yet easy to use and completely non-invasive, CCG may be a parallel tool to help indexing the probabilistic presentation of heart disease. Early detection of signs representing abnormalities of myocardial mechanical function or myocardial perfusion may later lead to further assessments aimed at lowering the risk of life-threatening events⁷⁻⁹.

We have concentrated here on comparative correlations between a series of time-domain indexes of LVH¹⁵⁻¹⁹ and echocardiographically measured MID^{20,21} to conclude that a frequency-domain index (4P sum in aVL; Figs. 1 and 2) performs better, especially when curvilinear fit is performed (Fig. 6). It is important to point out⁹ that aVL and V₃ are leads used in time domain to measure voltage and QRS duration to obtain the Cornell product¹⁷⁻¹⁹.

Although we have used a slightly modified cut-off value (145 instead of 125 g/m²) to index LVH echocardiographically^{20,21} and the sample group was quite limited, these preliminary observations point to a potential interest of CCG as a new tool to help indexing the probabilistic presentation of LVH. This conclusion thus reinforces previous observations whereby the

excellent predictive accuracy of this parameter was observed⁹.

Further studies are needed to enlarge the patient population and to investigate the mechanisms whereby the higher predictive accuracy of MID is obtained with frequency-domain analysis. It would be important to assess myocardial mass with nuclear magnetic resonance and to compare CCG data with magnetocardiography to obtain independent means of estimating both x and y values of the correlations. It may also be of interest to study pathological forms of LVH, such in hypertrophic cardiomyopathy and to compare with results obtained in physiological hypertrophy of athletes. Myocardial tissue characterization by echocardiography may contribute explanatory data.

Acknowledgments

The expert assistance of Alberto Lanza in obtaining the records of CCGs of this study is greatly appreciated. Dr. Bruno Malerba was instrumental in enabling us to perform the present investigation.

References

1. Surawicz B, Knilans TK. Chou's electrocardiography in clinical practice: adult and pediatric. 5th edition. Philadelphia, PA: WB Saunders, 2001: 3-27.
2. Fang DQ, Dong J, Feng GQ, Zhang S, Song Z. A study of the influence of industrial noise on information process of brain and ECG. *Kexue Tongbao* 1983; 28: 973-7.
3. Schreck DM, Ng L, Schreck BS, et al. Detection of coronary artery disease from the normal resting ECG using nonlinear mathematical transformation. *Ann Emerg Med* 1988; 17: 132-4.
4. Schreck DM, Terndrup TE, Bosco SF, Zacharias D, Ng L, Schreck BS. Correlation of nonlinear mathematical transformation of the normal electrocardiogram with the severity of coronary artery disease. *Crit Care Med* 1989; 17: 269-73.
5. Fischer JC. A potentially powerful new tool for non-invasive diagnosis of cardiac abnormalities: the CUPID[®] system for analysis of electrocardiograms in the frequency domain. *Biochem Instrument Technol* 1998; 32: 387-400.
6. Mroczka T, Lewandowski P, Maniewski R, Liebert A, Spioch M, Steinbach K. Effectiveness of high resolution ECG spectral analysis in discrimination of patients prone to ventricular tachycardia and fibrillation. *Med Sci Monit* 2000; 6: 1018-26.
7. Noera G, Oueida F. Cardiac ultra-phase information diagnosis (CUPID): nuove possibilità strumentali di diagnosi precoce della cardiopatia ischemica nell'anziano. *Giornale di Arteriosclerosi* 1999; 24: 81-4.
8. Weiss MB, Narasimhadevara SM, Feng GQ, Shen JT. Computer-enhanced frequency-domain and 12-lead electrocardiography accurately detect abnormalities consistent with obstructive and nonobstructive coronary artery disease. *Heart Dis* 2002; 4: 2-12.
9. Puddu PE, Schiariti M, Ciavarella GM, et al. Nuovi criteri di diagnostica dell'ipertrofia ventricolare sinistra basati sull'analisi delle basse frequenze in ultrafase. (abstr) *Ital Heart J* 2002; 3 (Suppl 7): 30S.
10. Chen BH, Tan TY, Li JM, Feng GQ, Ren BY, Fang DQ. Eight new biocybernetic indexes for evaluating brain function. Preliminary clinical application. *Chin Med J (Engl)* 1984; 97: 231-8.
11. Akay YM, Akay M, Welkowitz W, Semmlow JL, Kostis JB. Noninvasive acoustical detection of coronary artery disease: comparative study of signal processing methods. *IEEE Trans Biomed Eng* 1993; 40: 571-8.
12. Yambe T, Nitta S, Nanka S, et al. Spectral analysis of hemodynamics during left ventricular assistance. *Int J Artif Organs* 1996; 19: 367-71.
13. Akin M. Comparison of wavelet transform and FFT methods in the analysis of EEG signals. *J Med Syst* 2002; 26: 241-7.
14. Gular I, Hardalac F, Barisci N. Application of FFT analysed cardiac Doppler signals to fuzzy algorithm. *Comput Biol Med* 2002; 32: 435-44.
15. Sololow M, Lyon TP. The ventricular complex in left ventricular hypertrophy as obtained by unipolar precordial limb leads. *Am Heart J* 1949; 37: 152-9.
16. Lanti M, Puddu PE, Menotti A. Voltage criteria of left ventricular hypertrophy in sudden and nonsudden coronary artery disease mortality: the Italian section of the Seven Countries Study. *Am J Cardiol* 1990; 66: 1181-5.
17. Casale PN, Devereux RB, Alonso DR, Campo E, Kligfield P. Improved sex-specific criteria of left ventricular hypertrophy for clinical and computer interpretation of electrocardiograms: validation with autopsy findings. *Circulation* 1987; 75: 565-72.
18. Molloy TJ, Okin PM, Devereux RB, Kligfield P. Electrocardiographic detection of left ventricular hypertrophy by the simple QRS voltage-duration product. *J Am Coll Cardiol* 1992; 20: 1180-6.
19. Okin PM, Devereux RB, Jern S, et al, for the Losartan Intervention For Endpoint reduction in hypertension (LIFE) Study Investigators. Regression of electrocardiographic left ventricular hypertrophy by losartan versus atenolol: the Losartan Intervention for Endpoint reduction in Hypertension (LIFE) Study. *Circulation* 2003; 108: 684-90.
20. Devereux RB, Alonso DR, Lutas EM, et al. Echocardiographic assessment of left ventricular hypertrophy: comparison to necropsy findings. *Am J Cardiol* 1986; 57: 450-8.
21. Ganau A. Diagnosi di ipertrofia cardiaca e delle sue complicanze nel paziente iperteso. In: Ganau A, Saba PS, Roman MJ, Devereux RB, eds. *Ipertrofia del cuore e dei vasi nell'ipertensione*. Roma: Società Italiana di Cardiologia, 2002: 125-56.